

© 2021 Universidad Nacional Autónoma de México, Facultad de Estudios Superiores Zaragoza.
This is an Open Access article under the CC BY-NC-ND license (<http://creativecommons.org/licenses/by-nc-nd/4.0/>).
TIP Revista Especializada en Ciencias Químico-Biológicas, 24: 1-18, 2021.
<https://doi.org/10.22201/fesz.23958723e.2021.314>

In vitro and *in silico* biological evaluation of phthalimide derivatives as antiproliferative agents

Crystel A. Sierra-Rivera¹, Muhammad Kashi², Lenci K. Vázquez-Jiménez²,
Alejandro Zugasti-Cruz¹, Alfredo Juárez-Saldivar²,
Alma D. Paz-González² and Gildardo Rivera^{2*}

¹Laboratory of Immunology and Toxicology, Faculty of Chemistry, Autonomous University of Coahuila, Saltillo, Coahuila, 25280, México. ²Laboratorio de Biotecnología Farmacéutica, Centro de Biotecnología Genómica, Instituto Politécnico Nacional, Reynosa, 88710, Tamaulipas, México.
E-mail: *gildardors@hotmail.com

ABSTRACT

Phthalimide is considered a scaffold for the development of new anticancer agents. In this work, the antiproliferative activity of forty-three phthalimide derivatives was evaluated against cervical (HeLa), liver (HepG2), breast (4T1) cancer cell lines, and a normal cell line of murine fibroblasts (3T3). Finally, a molecular docking analysis of phthalimide derivatives on the active site of the enzymes DNA methyltransferase 1 (DNMT1) and vascular endothelial growth factor receptor 2 (VEGR2) as potential drug targets was performed. The compounds, C16, E11, and E16 showed the best antiproliferative activity against the cell lines HeLa and 4T1. Only, the compound H16 decreased 32% cell proliferation against HepG2 cell line. The compounds H5, H16, E2, E16, and C1 did not affect the proliferation of the 3T3 cell line. The molecular docking analysis showed that phthalimide derivatives have a greater affinity for DNMT1 than S-adenosyl-L-homocysteine, a potent DNMT1 inhibitor. However, molecular docking results do not correlate with their antiproliferative effects, suggesting another potential mechanism of action for the active compounds.

Keywords: antiproliferative, DNA methyltransferase 1, molecular docking, phthalimide.

Evaluación biológica *in vitro* e *in silico* de derivados de ftalimida como agentes antiproliferativos

RESUMEN

La estructura de la ftalimida es considerada un bloque de construcción para el desarrollo de nuevos agentes anticancerígenos. En este trabajo, se evaluó la actividad antiproliferativa de cuarenta y tres derivados de ftalimida contra las líneas celulares cancerígenas de cérvix (HeLa), hígado (HepG2), mama (4T1), y la línea celular normal de fibroblastos murinos (3T3). Por último, se realizó un análisis de acoplamiento molecular de los derivados de la ftalimida en el sitio activo de la enzima metiltransferasa 1 de DNA (DNMT1, por sus siglas en inglés) y el receptor del factor de crecimiento endotelial vascular 2 (VEGR2, por sus siglas en inglés) como posibles blancos farmacológicos. Los compuestos C16, E11 y E16 mostraron la mejor actividad antiproliferativa contra las líneas celulares HeLa y 4T1. Solamente, el compuesto H16 disminuyó 32% la proliferación celular de la línea HepG2. Los compuestos H5, H16, E2, E16 y C1 no afectaron la proliferación celular de la línea 3T3. El análisis de acoplamiento molecular demostró que los derivados de la ftalimida tienen una mayor afinidad que la S-adenosil-L-homocisteína, un potente inhibidor de la metiltransferasa 1 de DNA. Sin embargo, los resultados del acoplamiento molecular no se correlacionan con los efectos antiproliferativos; lo cual sugiere que los compuestos activos tienen otro mecanismo de acción.

Palabras clave: antiproliferativo, metiltransferasa 1 de ADN, acoplamiento molecular, ftalimida.

INTRODUCTION

Cancer is one of the main causes of morbidity and mortality worldwide. According to the World Health Organization, 9.6 million cancer deaths were reported in 2018, making it an important public health concern. Lung, prostate, and liver cancer are among the most prevalent in men and liver cancer is the second most common cause of death from cancer. Breast, cervical and thyroid cancer are among the most prevalent in women. In 2018, over 500,000 and 2 million of cases of cervical and breast cancer, respectively, were reported (WHO, 2019).

Cancer treatment commonly includes chemotherapy and radiotherapy; however, the anticancer drugs available have low selectivity and cause severe adverse effects, such as nephrotoxicity, neurotoxicity, and myelosuppression (Matsuo Lin, Roman & Sood, 2010). Therefore, the design and development of compounds as new anticancer agents against the types of cancer with the highest incidence are of vital importance in the area of health. In this sense, heterocyclic derivatives, such as quinoxaline (Kamal Bolla, Srikanth & Srivastava, 2013; Rivera *et al.*, 2017a; Rivera *et al.*, 2017b), uracil (Lu., Li, Mohamed, Wang & Meng, 2019), pyrimidines (Kilic-Kurt Bakar-Ates, Karakas & Kütük, 2018; Abdelhaleem., Abdelhameid, Kassab & Kandeel, 2018), β -lactams (Olazarán-Santibáñez, Bandyopadhyay, Carranza-Rosales, Rivera & Balderas-Rentería., 2017a; Olazarán *et al.*, 2017b), and phthalimide (Bailey *et al.*, 2003; Li *et al.*, 2011) are used to obtain new anticancer agents (Figure 1).

Phthalimide (Figure 2.A) derivatives are promising compounds for the development of new anticancer agents (Li *et al.*, 2011; Grigalius & Petrikaite, 2017; Kamal, Reddy, Reddy & Ramesh, 2002). However, the first step in knowing their potential as anticancer agents to determine their biological effects against cancer cell lines; for example, Bailey *et al.* obtained the phthalimide derivatives B and C (Figure 2.B and 2.C) with half-maximal inhibitory concentration (IC_{50}) values of 0.6 μ M and 4.9 nM, respectively, against CEM human leukemia cells (Bailey *et al.*, 2003). Afterward, Al-Soud & Al-Masoudi (2001), reported compound D (Figure 2.D), a phthalimide derivative with 61% growth inhibition against the SF-268 glioblastoma cell line (Chen *et al.*, 2010). Subsequently, Li *et al.* (2011) found that compound E (Figure 2.E) had higher IC_{50} values than the reference drug amonafide against the cancer cell lines MCF-7, HeLa, and 7721 (0.32, 1.02 and 0.46 μ M versus 1.68, 1.73 and 4.27 μ M, respectively).

The mechanism of action of phthalimide derivatives as anticancer agents includes different drug targets, such as methyltransferases (Mai & Altucci, 2009; Asgatay *et al.*, 2014), vascular endothelial growth factor receptor 2 (VEGR2) (Zahran *et al.*, 2014; Othman, Gad-Elkareem, El-Naggar, Nossier & Amr, 2019; Philoppes & Lamie, 2019), lipoxygenases (LOX) (Aliabadi *et al.*, 2015) fibroblast growth factor receptors (FGFRs) (Sundaresan *et al.*, 2019) and topoisomerase II (Xie *et al.*, 2011; Miyachi, Ogasawara, Azuma & Hashimoto, 1997; Yu & Wang, 2008). In the first decade of 2000, methyltransferases were reported as a promising target for cancer therapy (Siedlecki *et al.*,

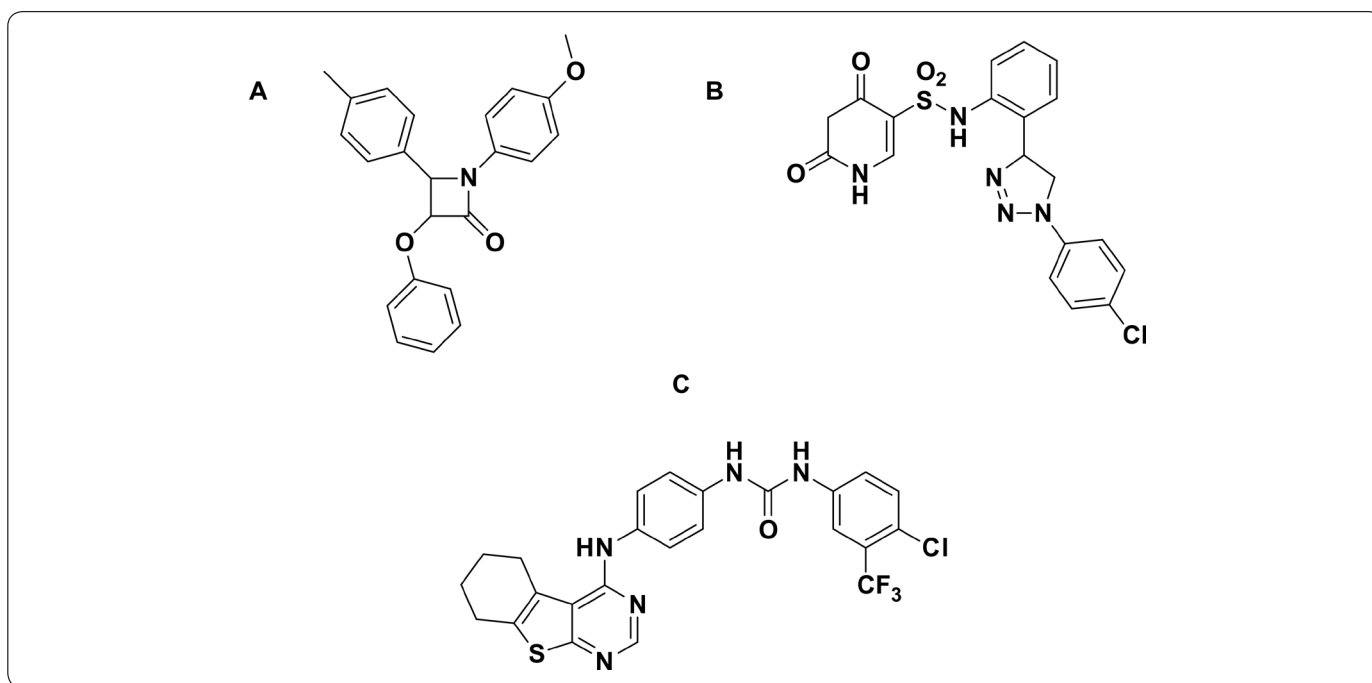


Figure 1. Chemical structures of compounds (A: β -lactam; B: uracil; and C: pyrimidin derivatives) with anticancer activity. Figure designed by the authors.

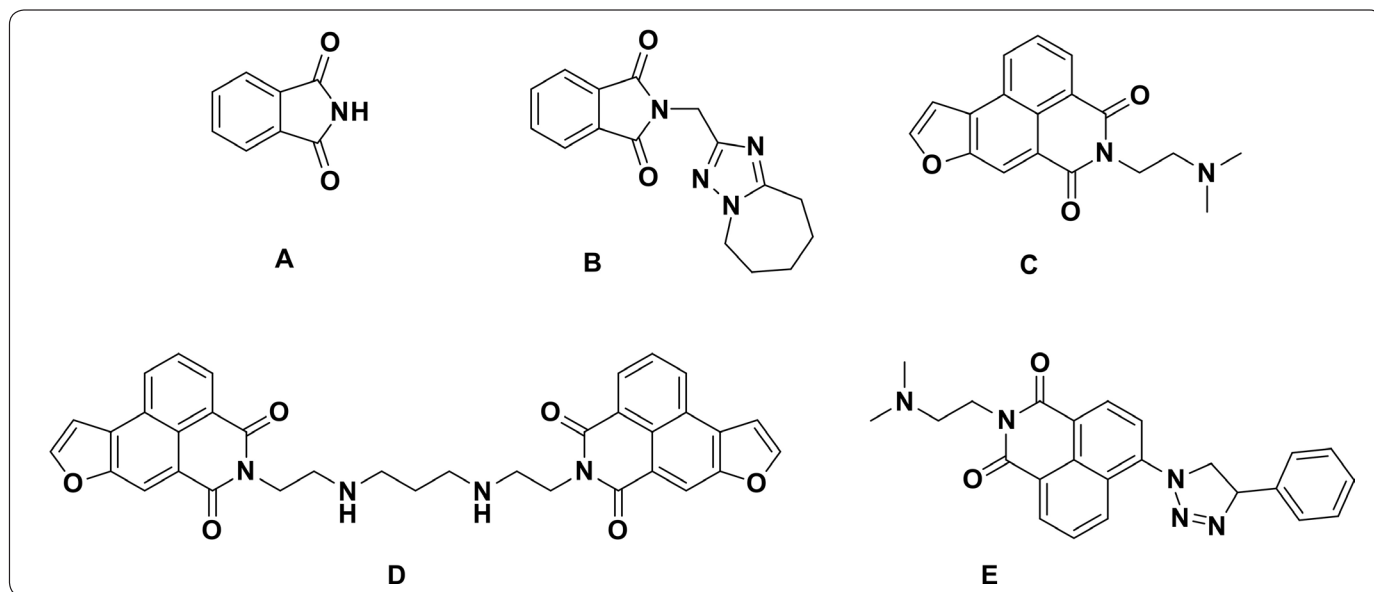


Figure 2. Chemical structure of phthalimide (A) and phthalimide analogs (B-E) with anticancer activity. Figure designed by the authors.

2006) and VEGFR2 has been associated in *in silico* analyses with the biological effects of phthalimide derivatives. Based on the above, this work aimed to evaluate the antiproliferative activity of forty-three phthalimide derivatives against one main cancer cell line in men (HepG2) and two main cancer cell lines in women (HeLa, and 4T1). Additionally, the cytotoxicity of compounds against a normal murine fibroblast cell line (3T3) was determined. Finally, to determine their potential mechanism of action, a molecular docking analysis was done on the active site of two enzymes (DNMT1 and VEGFR2) reported as the main potential phthalimide targets.

MATERIALS AND METHODS

Chemistry

A total of forty-three phthalimide derivatives were obtained following the procedure reported by Kashif *et al.*, (2018). The structural elucidation by infrared (IR) and proton nuclear magnetic resonance (¹H-NMR) was done (Supplementary material).

Cell culture

The human cervical cancer (HeLa), human liver (HepG2), murine breast carcinoma (4T1) and murine fibroblasts (3T3) cell lines they were obtained from the American Type Culture Collection (ATCC, Manassas, VA, USA). Cell lines were cultured in modified Dulbecco's Eagle's medium (DMEM/F-12) supplemented with 10% fetal bovine serum (FBS) and 1% antibiotic-antifungal solution (Sigma Aldrich, ST. Louis, MO).

Evaluation of proliferative activity by MTT

HeLa, HepG2, 4T1, and 3T3 cell lines were cultured at 5×10^3 cells/well, using flat-bottom 96 well plates and incubated

overnight at 37 °C and 5% CO₂. After, all phthalimide derivatives and doxorubicin (DOX) were added at 20 μg/mL (In Table I, the concentration for each compound were converted to micromolar units) previously diluted in DMEM/F-12 culture medium. Subsequently, the culture plates were incubated for 72 h. After this incubation, 20 μL of MTT/well (Sigma, St. Louis, MO, USA) was added to a final concentration of 5 mg/mL to quantify the percentage of proliferation. After 4 h of incubation, the supernatants were discarded and 100 μL dimethyl sulfoxide (DMSO) was added to each well to dissolve formazan crystals. Finally, measured at a wavelength of 540 nm using a Microplate Spectrophotometer (BioTek Instruments, Inc., Winooski, VT, USA). The percentage of cell proliferation was obtained through the following formula: Cell proliferation (%) = (Absorbance of treated cells/Absorbance of control cells) X 100.

Molecular docking analysis

A molecular docking analysis of phthalimide derivatives on the active site of human DNMT1 and VEGFR2 was performed using the software AutoDock Vina 1.1.2 (Trott & Olson, 2010). The crystallographic structures of DNMT1 in complex with *S*-adenosyl-1-homocysteine (SAH) and VEGFR2 in complex with methyl (5-{4-[(2-fluoro-5-(trifluoromethyl)phenyl]amino}carbonyl)amino]phenoxy}-1*h*-benzimidazol-2-yl) carbamate (GIG) were retrieved from the Protein Data Bank (www.rcsb.org, PDB ID: 3PTA and 2OH4, respectively). The structure of both proteins was prepared using the Dock Prep tool of the software UCSF Chimera (Pettersen *et al.*, 2004), which removes all ligands and water molecules of the receptor structure, also repairs missing side chains and adds polar hydrogens. Meanwhile, the co-crystallized ligands (SAH and GIG) and the phthalimide derivatives were prepared using Open

Babel (O'Boyle *et al.*, 2011); this tool minimized the structures of each ligand and adds polar hydrogens to them. Ligands and the receptor were converted to pdbqt format using MGLTools 1.1.6 (Morris *et al.*, 2009). The docking search space had values of size X= 20, Y= 20, and Z= 20 and was centered according to the coordinates of the co-crystallized ligand in the PDB file. The non-covalent interactions of the docking results were calculated using Protein-Ligand Interaction Profiler (PLIP) (Salentin, Schreiber, Haupt, Adasme & Schroeder, 2015).

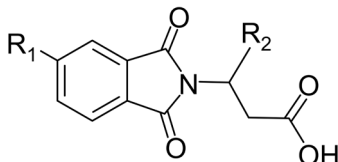
RESULTS AND DISCUSSION

Antiproliferative activity

The results obtained from the evaluation of forty-three phthalimide derivatives against cell lines of the main types of cancer that cause mortality and normal cell lines to validate the selectivity of the biological effect of the phthalimide derivatives at one concentration are shown in Table I and graphics 1-4. DOX was used a positive control. This drug is a chemotherapeutic agent with antiproliferative and cytotoxic effects, commonly used in various types of human cancer and biological models (Al-Abbasi *et al.*, 2016).

Graphic 1 show that compounds from series H have a low effect on decreasing HeLa proliferation (0-15%), although, compounds H11 and H5, H9, and H13 show naphthyl and nitro groups that have been previously relationated with biological effects in anticancer agents, while the positive control DOX decreased cell proliferation by 84.06%. In general, the compounds from the second series E, with a methyl group on the phthalimide ring, significantly decreased HeLa cell proliferation, except for compounds E5, E7, and E8. Compounds E1, E11, E12, and E16 decreased HeLa cell proliferation by around 40%. These results indicate that the incorporation of a methyl group at 5-position on the phthalimide ring enhances their biological effect. Replacement of methyl by a carboxylic group in compounds of series C had a similar biological behavior on HeLa cells. Compounds C7, C8, and C16 significantly decreased the proliferation of the HeLa cell line (36.33, 40.21, and 40.37%, respectively). Interestingly, the compounds E16 and C8 not showed cytotoxic effects (proliferation percentage of around 96 and 87%, respectively) against the normal cell line (3T3) (Graphic 4) suggesting selectivity against the HeLa cell line. This antiproliferative activity from phthalimide

Table I. Biological effect (percentage cell proliferation) of phthalimide derivatives against cervical (HeLa), liver (HepG2) and breast (4T1) cancer and normal (3T3) cell lines at one concentration.

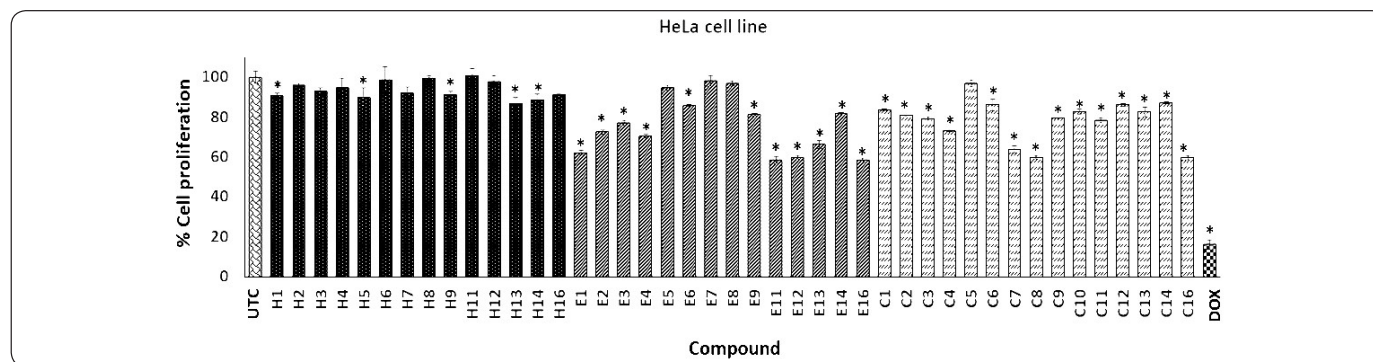


Compound	R1	R2	Concentration (µM)	% Cell proliferation ± SD Panel/Cell Line			
				HeLa	HepG2	4T1	3T3
UTC	--	--	--	100.00 ± 3.00	100.00 ± 0.70	100.00 ± 1.01	100.00 ± 0.91
H1	H	C ₆ H ₅ pOCH ₃	61.47	90.59 ± 1.32*	99.18 ± 2.31	49.57 ± 2.09*	62.33 ± 2.19*
H2	H	C ₆ H ₅ pCH ₃	64.65	96.18 ± 0.50	90.52 ± 0.52*	98.13 ± 4.53	65.91 ± 1.48*
H3	H	C ₆ H ₅ pCH ₂ CH ₃	61.85	92.88 ± 1.68	91.54 ± 0.97*	84.64 ± 0.40*	60.53 ± 1.27*
H4	H	C ₆ H ₅ pOH	64.24	94.74 ± 4.60	97.04 ± 2.36	84.83 ± 0.40*	67.26 ± 3.53*
H5	H	C ₆ H ₅ pNO ₂	58.77	89.95 ± 4.55*	88.69 ± 2.00*	86.20 ± 1.44*	95.96 ± 3.39
H6	H	C ₆ H ₅ pF	63.84	98.73 ± 6.63	76.45 ± 2.64*	97.61 ± 3.80	78.02 ± 3.53*
H7	H	C ₆ H ₅ pCl	60.65	92.20 ± 2.84	84.61 ± 2.51*	91.31 ± 8.94*	43.94 ± 3.53*
H8	H	C ₆ H ₅ pBr	53.44	99.66 ± 1.23	89.19 ± 0.85*	98.55 ± 3.51	68.16 ± 0.70*
H9	H	C ₆ H ₃ oNO ₂ O ₂ C ₂ H ₄	50.20	91.26 ± 1.59*	100.0 ± 0.45	85.20 ± 1.75*	69.05 ± 0.21*
H11	H	C ₁₀ H ₇	57.91	100.85 ± 3.49	90.11 ± 0.85*	75.09 ± 0.86*	48.87 ± 3.81*
H12	H	C ₆ H ₄ pC ₆ H ₅	53.85	97.71 ± 3.30	84.51 ± 1.10*	98.61 ± 4.61	24.21 ± 0.91*
H13	H	C ₆ H ₅ oNO ₂	58.77	86.77 ± 3.23*	87.36 ± 1.16*	75.52 ± 1.20*	81.16 ± 0.77*
H14	H	C ₄ H ₃ O	70.11	88.55 ± 2.94*	82.87 ± 0.88*	85.97 ± 2.72*	61.43 ± 0.21*
H16	H	C ₄ H ₃ S	66.37	91.26 ± 0.35	68.09 ± 2.36*	94.01 ± 4.50	94.61 ± 0.21
E1	CH ₃	C ₆ H ₅ pOCH ₃	58.93	62.07 ± 1.10*	99.24 ± 0.85	96.34 ± 4.53	47.98 ± 1.48*
E2	CH ₃	C ₆ H ₅ pCH ₃	61.85	72.42 ± 1.15*	90.52 ± 2.28*	99.06 ± 2.20	95.51 ± 1.27

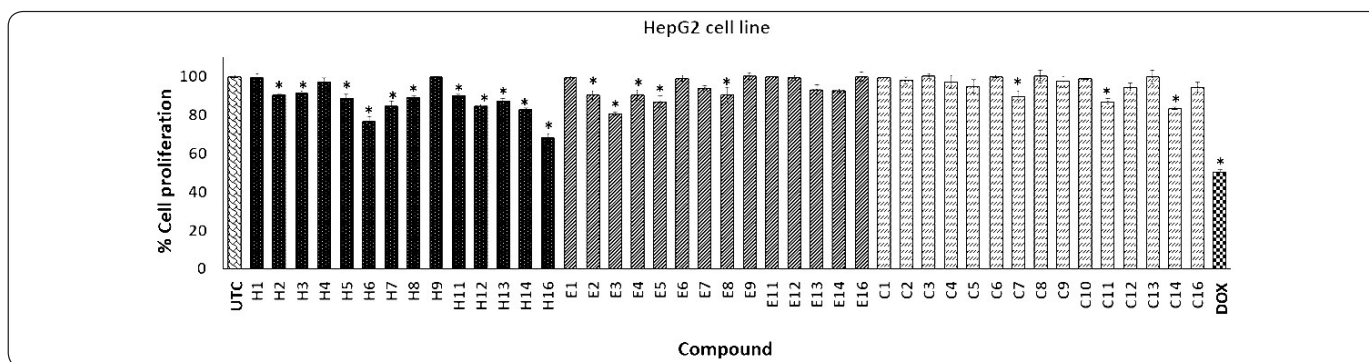
Table I. Biological effect (percentage cell proliferation) of phthalimide derivatives against cervical (HeLa), liver (HepG2) and breast (4T1) cancer and normal (3T3) cell lines at one concentration.

Compound	R1	R2	Concentration (µM)	% Cell proliferation ± SD Panel/Cell Line			
				HeLa	HepG2	4T1	3T3
E3	CH ₃	C ₆ H ₅ pCH ₂ CH ₃	59.28	77.23 ± 1.32*	80.65 ± 1.00*	98.89 ± 1.63	65.02 ± 0.70*
E4	CH ₃	C ₆ H ₅ pOH	61.47	70.50 ± 0.90*	90.52 ± 2.75*	97.61 ± 3.18	90.58 ± 1.13*
E5	CH ₃	C ₆ H ₅ pNO ₂	56.44	94.59 ± 1.21	86.85 ± 3.26*	82.52 ± 3.25*	65.47 ± 0.49*
E6	CH ₃	C ₆ H ₅ pF	61.10	85.76 ± 0.51*	98.98 ± 1.51	98.80 ± 4.3	69.95 ± 1.42*
E7	CH ₃	C ₆ H ₅ pCl	58.18	98.25 ± 2.65	94.09 ± 1.36	80.43 ± 4.03*	62.33 ± 3.46*
E8	CH ₃	C ₆ H ₅ pBr	51.51	96.73 ± 1.33	90.32 ± 4.23*	100.64 ± 2.62	59.19 ± 0.07*
E9	CH ₃	C ₆ H ₃ oNO ₂ O ₂ C ₂ H ₄	48.50	81.26 ± 0.75*	100.31 ± 1.67	93.38 ± 4.20	50.67 ± 0.35*
E11	CH ₃	C ₁₀ H ₇	55.65	58.42 ± 1.65*	100.0 ± 0.36	51.25 ± 0.30*	78.47 ± 1.90*
E12	CH ₃	C ₆ H ₄ pC ₆ H ₅	51.89	60.02 ± 0.89*	99.39 ± 1.32	91.11 ± 2.62*	78.47 ± 1.69*
E13	CH ₃	C ₆ H ₅ oNO ₂	56.44	66.26 ± 1.83*	93.27 ± 2.60	95.77 ± 2.55	64.57 ± 1.34*
E14	CH ₃	C ₄ H ₃ O	66.82	81.87 ± 0.40*	92.56 ± 1.10	50.20 ± 1.04*	77.57 ± 0.42*
E16	CH ₃	C ₄ H ₃ S	63.42	58.57 ± 0.64*	99.90 ± 2.51	51.23 ± 0.66*	96.86 ± 4.17
C1	COOH	C ₆ H ₅ pOCH ₃	54.15	83.78 ± 0.41*	99.54 ± 0.15	98.26 ± 2.80	104.03 ± 0.70
C2	COOH	C ₆ H ₅ pCH ₃	56.60	80.81 ± 0.15*	97.96 ± 1.66	75.04 ± 1.24*	69.05 ± 3.25*
C3	COOH	C ₆ H ₅ pCH ₂ CH ₃	54.44	79.44 ± 0.55*	100.20 ± 1.42	53.59 ± 2.65*	79.82 ± 1.55*
C4	COOH	C ₆ H ₅ pOH	56.29	73.04 ± 0.30*	96.94 ± 3.53	50.26 ± 0.62*	68.60 ± 0.49*
C5	COOH	C ₆ H ₅ pNO ₂	52.04	96.96 ± 1.85	94.90 ± 3.75	98.18 ± 3.15	68.16 ± 1.69*
C6	COOH	C ₆ H ₅ pF	53.51	86.21 ± 2.82*	100.0 ± 0.60	73.02 ± 2.10*	59.19 ± 0.56*
C7	COOH	C ₆ H ₅ pCl	55.97	63.67 ± 1.85*	89.60 ± 3.21*	58.18 ± 1.49*	60.08 ± 2.54*
C8	COOH	C ₆ H ₅ pBr	47.82	59.79 ± 0.73*	100.15 ± 3.25	67.96 ± 2.86*	87.44 ± 1.48*
C9	COOH	C ₆ H ₃ oNO ₂ O ₂ C ₂ H ₄	45.21	79.51 ± 0.26*	97.55 ± 2.88	64.84 ± 2.81*	80.71 ± 1.13*
C10	COOH	C ₆ H ₃ O ₂ C ₂ H ₄	51.21	82.79 ± 1.15*	98.93 ± 0.55	100.54 ± 4.16	83.85 ± 0.63*
C11	COOH	C ₁₀ H ₇	48.14	78.37 ± 1.47*	86.95 ± 1.61*	92.87 ± 2.06	71.30 ± 1.34*
C12	COOH	C ₆ H ₅ pC ₆ H ₅	52.04	86.14 ± 0.79*	94.60 ± 1.88	92.87 ± 4.58	71.74 ± 0.14*
C13	COOH	C ₆ H ₅ oNO ₂	52.04	82.56 ± 2.28*	99.80 ± 3.48	55.53 ± 0.37*	60.98 ± 1.69*
C14	COOH	C ₄ H ₃ O	60.74	87.28 ± 0.43*	83.49 ± 0.55*	50.14 ± 0.77*	60.53 ± 0.98*
C16	COOH	C ₄ H ₃ S	57.91	59.63 ± 1.01*	94.29 ± 2.69	50.19 ± 0.62*	72.64 ± 1.76*
DOX	-	-	36.79	15.94 ± 2.60*	50.37 ± 1.53*	55.14 ± 0.96*	40.97 ± 1.88*

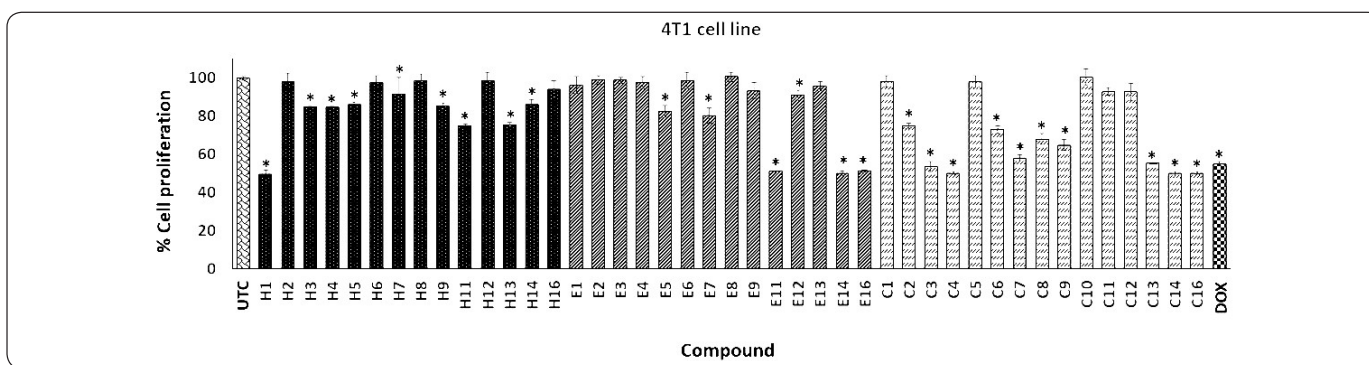
^aData represent the means of triplicate samples with ± SD indicated. **p* < 0.05 as compared with untreated cells (UTC).



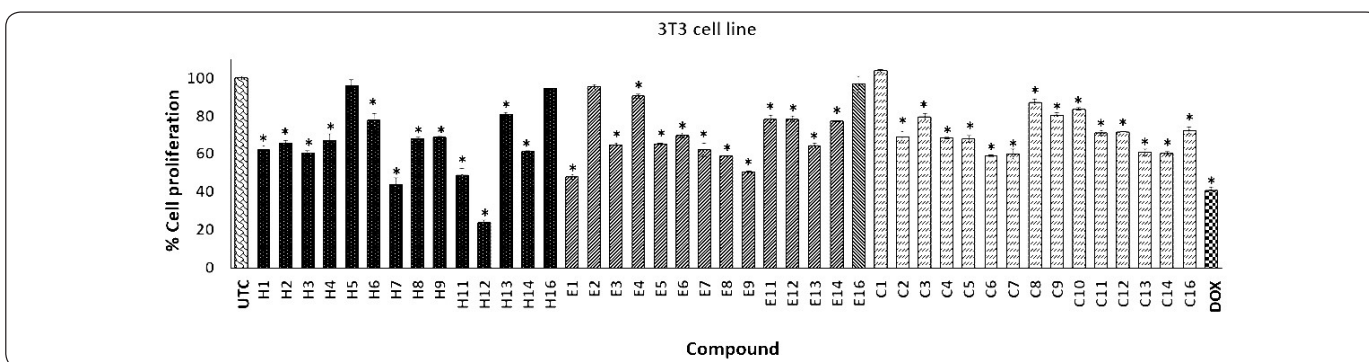
Graphic 1. Effect of phthalimide derivatives against HeLa cell line. Cervical cancer cells were treated with phthalimide derivatives and incubated for 72 h at 37 °C. Thereafter, an MTT assay was performed. The optical density was measured at 540 nm. Data represent the means of triplicate samples with ± SD indicated. **p* < 0.05 as compared with untreated cells. Figure prepared by the authors.



Graphic 2. Effect of phthalimide derivatives against HepG2 cell line. Hepatocarcinoma cells were treated with phthalimide derivatives and incubated for 72 h at 37 °C. Thereafter, an MTT assay was performed. The optical density was measured at 540 nm. Data represent the means of triplicate samples with ± SD indicated. **p* < 0.05 as compared with untreated cells. Figure prepared by the authors.



Graphic 3. Effect of phthalimide derivatives against 4T1 cell line. Breast cancer cells were treated with phthalimide derivatives and incubated for 72 h at 37 °C. Thereafter, an MTT assay was performed. The optical density was measured at 540 nm. Data represent the means of triplicate samples with ± SD indicated. **p* < 0.05 as compared with untreated cells. Figure prepared by the authors.



Graphic 4. Effect of phthalimide derivatives against 3T3 cell line. Murine fibroblast cells were treated with phthalimide derivatives and incubated for 72 h at 37 °C. Thereafter, an MTT assay was performed. The optical density was measured at 540 nm. Data represent the means of triplicate samples with ± SD indicated. **p* < 0.05 as compared with untreated cells. Figure prepared by the authors.

derivatives on HeLa cell lines has been reported by Shiheido *et al.*, (2012) They found that phthalimide derivatives such as 2-(2,6-diisopropyl phenyl)-5-amino-1H-isoindole-1,3-dione (TC11) inhibited cell proliferation of multiple myeloma lines (KMM1, KMM11, KMS27, KMS34, and RPMI8226) and induced caspase-mediated apoptosis on KMS34 and HeLa cell lines at a concentration of 50 μM.

Series H on HepG2 showed a low effect on the proliferative cell. Although, compound H16, with the thienyl group, decreased cell proliferation by 31.91% with a low effect (6%) on the 3T3 cell line. Subsequently, the incorporation of methyl or a carboxylic group on the phthalimide ring (series E and C, respectively) did not affect biological activity on the HepG2 cell line. In this same cell line, DOX decreased cell

proliferation by 49.63% (Graphic 2). Similar to our results, Zahran *et al.*, (2014) determined that the HepG2 cell line treated with phthalimide ester analogs after 48 h of incubation showed a moderate cytotoxic effect against the MCF-7 breast cancer cell line.

On the other hand, series H on 4T1 cells showed a null or low antiproliferative effect, except compound H1 (50.43%) (Graphic 3); however, these compounds also reduced the proliferative effect in normal cells (3T3) (Graphic 4). The incorporation of a methyl group on the phthalimide group reduced the antiproliferative effect (E1 with 99.24%). Graphic 3 shows that compounds E11, E14, and E16 on the 4T1 cell line demonstrated antiproliferative activity (47.75, 49.80, and 49.77%, respectively). Interestingly, E16 showed a low effect on normal 3T3 cells. These results indicate that E16 showed a selective effect by reducing proliferation in HeLa and 4T1 cells without significantly affecting the proliferation of 3T3 cells (Graphics 1, 3, and 4). Finally, series C against the 4T1 cell line showed the best results. Compounds C3, C4, C14, and C16 produced a good antiproliferative effect (from 45 to 50%). However, these compounds also affected the 3T3 cell line. DOX causes a decrease of 44.86% in cell proliferation against 4T1, and 59.03% against the 3T3 cell line. These results were similar to those obtained by Zahran *et al.*, (2014) in which a macrophage cell line (RAW 267.7) was treated with 12.5 $\mu\text{g/mL}$ of bis-phthalimide during 48 h of incubation, finding a cytotoxic effect of around 40%.

In summary, the results show that the HepG2 cancer cell line was the most resistant and that 4T1 was the most sensitive cancer cell line to the phthalimide derivatives evaluated. On the other hand, HeLa was more sensitive and 4T1 more resistant to DOX treatment (15.94% and 40.97% of cell proliferation, respectively).

Molecular docking analysis on DNA methyltransferase 1

To know the potential mechanism of action of phthalimide derivatives, a molecular docking analysis on the active site of DNMT1 with SAH and phthalimide derivatives was done. First, the non-covalent interactions in the crystallographic structure of the DNMT1-SAH complex (PDB ID: 3PTA) were calculated with protein-ligand interaction profiler (PLIP). As Figure 3 shows, nine hydrogen bonds were identified. These interactions show that the pyrimidine ring of SAH plays an important role in the binding to DNMT1 interacting with Met-1169, Asp-1190, and Cys-1191 through both of its nitrogens. In addition, the amine group attached to this ring interacts with the carboxyl group of Asp-1190. Another interesting subset of interactions are formed by Ser-1146, Gly-1150, and Leu-1151 with an oxygen atom of the carboxyl group of SAH. The rest of the hydrogen bonds are formed with Asn-1578 and Ala-1579. This complex was also analyzed by docking to reproduce the crystallographic pose of SAH. The DNMT1-SAH-docked complex with the

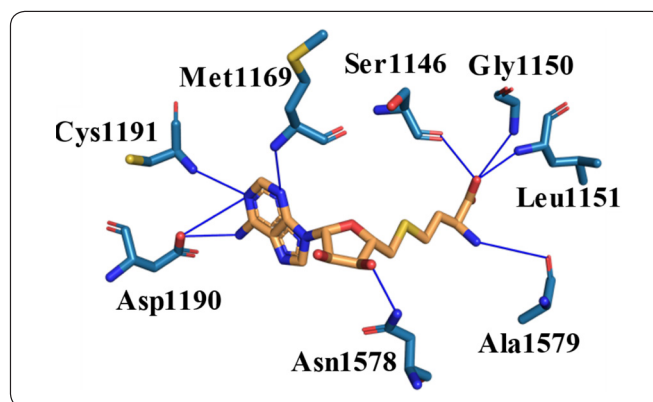


Figure 3. Non-covalent interactions between SAH and DNMT1. Hydrogen bonds are shown as blue lines. Figure designed by the authors.

lowest vina score (-8.0 kcal/mol) had an RMSD of 1.603; an RMSD lower than 2 is generally considered adequate *in silico* reproduction.

The binding modes of the phthalimide derivatives were evaluated by molecular docking using vina. The poses with the lowest free energy of binding of each compound were selected and ranked. All the phthalimide derivatives showed an equal or greater binding affinity than SAH (≥ -8.0 kcal/mol). Table II shows the top ten compounds and highlights the structures that have lower free energy of binding. Biphenyl and naphthalene groups, as well as the benzodioxine group, were among the best-ranked compounds. These groups tend to generate hydrophobic interactions and stacking with the aromatic residues, Phe-1145 and Trp-1170, amino acids on the binding site of DNMT1. Four compounds from series C are in the top ten, maybe due to their extra carboxyl group, which can form hydrogen bonds easily.

To understand the affinity of these phthalimide derivatives with DNMT1, non-covalent interactions were calculated with PLIP. The compound with the lowest free energy of binding was C-12 (-10.5 kcal/mol), which forms hydrogen bonds with Gly-1150, Leu-1151, and Asn-1578, the same as SAH. There were also interactions with Glu-698, Cys-1148, Gly-1149, and Val-1580 via hydrogen bond. In addition to these interactions, the biphenyl group of C-12 has hydrophobic interactions with Phe-1145, Met-1168, Pro-1225, and Leu-1247. In addition, one of the rings of this biphenyl group forms a π -stacking with Phe-1145. This π -stacking interaction is also present in E12, which also has a free energy of binding of -10.5 kcal/mol, even with the loss of hydrogen bonds due to the lack of a carboxyl group. C12 and E12 also shared hydrophobic interactions with Met-1169 and Pro-1225 and the hydrogen bond with ASN-1578. Interestingly, H12, which lacks the methyl group of E12, has a free energy of binding of -10.0 kcal/mol and four of its five interactions are the same in C12 and E12. These interactions are highlighted in Figure 4.

Table II. The top ten (free energy binding) of phthalimide derivatives on active site of DNMT1.

Compound	Structure	Vina Score (kcal/mol)
SAH		-8.0
C12		-10.5
E12		-10.5
C11		-10.4
E8		-10.3
E11		-10.3

Compound	Structure	Vina Score (kcal/mol)
C8		-10.1
H12		-10.0
H11		-9.7
H8		-9.6
C10		-9.5

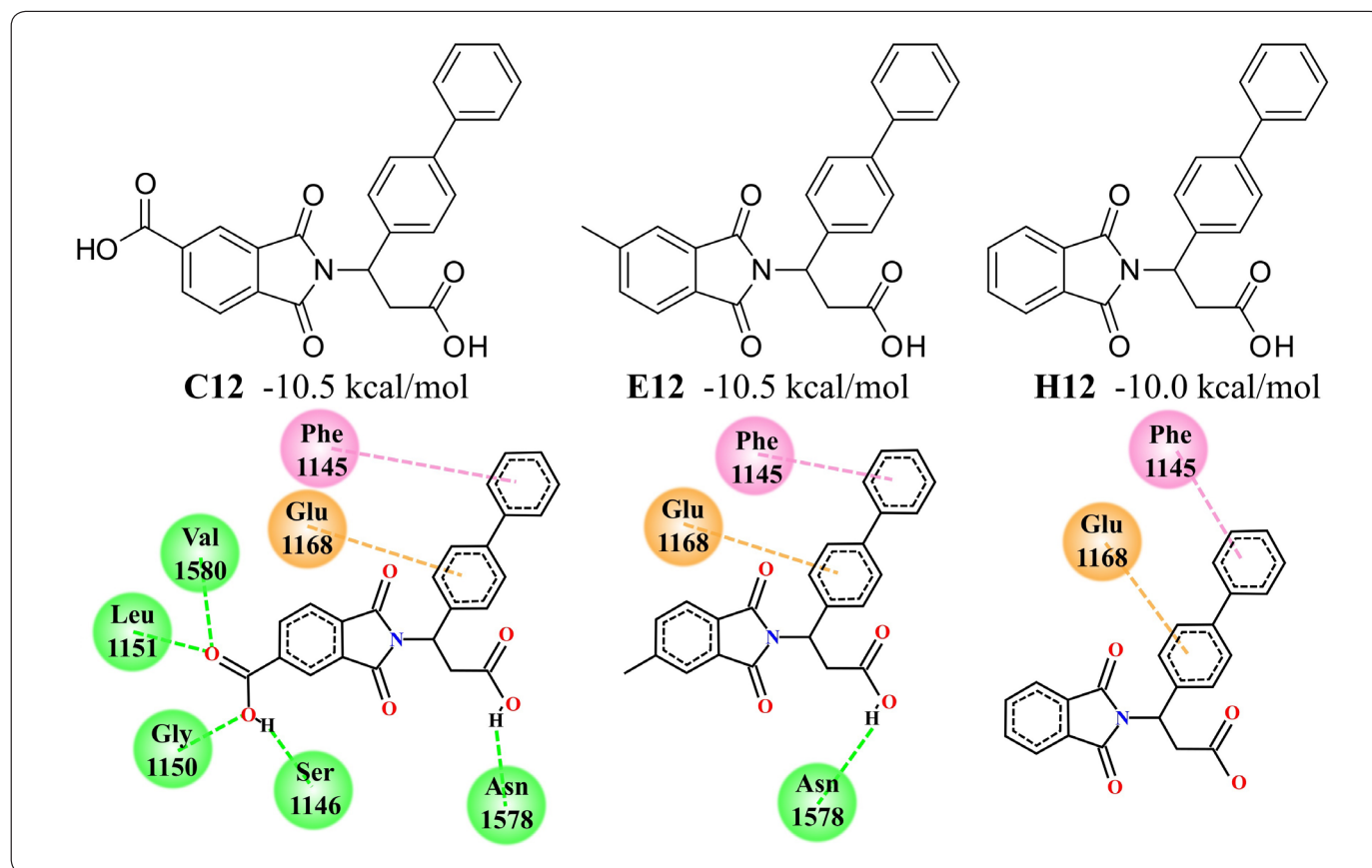


Figure 4. Structure and interactions of the compounds C12, E12 and H12 with a biphenyl group on the active site of DNMT1. This substructure showed to be the main source of energetic contribution to the affinity of the phthaloyl derivatives with DNMT1. Interactions are shown in green for hydrogen bonds, pink for π -stacking and orange for cation- π . Figure designed by the authors.

Another substructure of interest is the naphthalene group of C11 (-10.4 kcal/mol), E11 (-10.3 kcal/mol), and H11 (-9.7 kcal/mol), which keeps the π -stacking with Phe-1145 and hydrophobic interaction with Pro-1125 like the biphenyl group. These observations indicate that π -stacking interaction provides the greatest energy contribution. Another important contribution is by hydrogen bonds, in the comparison of interactions of H12 (-10.0 kcal/mol) and H11A (-9.7 kcal/mol), the only difference is a hydrogen bond with Asn-1578 of H12. Interestingly, benzodioxane does not generate π -stacking with Phe-1145 like biphenyl and naphthalene, nevertheless, the nitro group forms a hydrogen bond with Gly-1223 and Glu-1266, an interaction not present in other complexes. In conclusion, *in silico* calculations show that phthalimide derivatives interact with a higher affinity than SAH, a potent DNMT1 inhibitor. Non-covalent interactions of docked complexes point to a different inhibition mechanism between SAH and the phthalimide derivatives. In addition, it was noted that carboxyl and nitro groups contribute to binding through hydrogen bond formation, as well as biphenyl and naphthalene groups with π -stacking with Phe-1145. However, the antiproliferative activity from phthalimide

derivatives is not related with binding on the active site of DNMT1; therefore, these results could suggest two options: phthalamide derivatives have low membrane permeability or they have another potential drug target.

Molecular docking analysis on VEGFR2

Previously, VEGFR2 a kinase receptor involved in angiogenesis has been propose as a drug target from phthalimide derivatives with anticancer activity using molecular docking (Othman *et al.*, 2019). Therefore, in this study VEGFR2 was considering as a potential drug target. The 2HO4 pdb structure shows VEGFR2 in complex with GIG. The non-covalent interactions in this complex were calculated using the PLIP tool. Most of these interactions are hydrophobic and involved the residues Val846, Ala864, Lys866, Ile886, Ile890, Val897, Val914, Leu1033, Asp1044, and Phe1045. This complex also shows hydrogen bonding with Glu883, Cys917, and Gly920. To compare this complex with the possible binding mechanism of phthalimide derivatives, the molecular docking approach was applied first to GIG, obtaining a score of -10.4 kcal/mol, and then to the phthalimide derivatives. Table III shows the structure and score of the top ten compounds based on their vina score.

Table III. The top ten (free energy binding) of phthalimide derivatives on active site of VEGFR2.

Compound	Structure	Vina Score (kcal/mol)	Compound	Structure	Vina Score (kcal/mol)
GIG		-10.4	E5		-8.9
C12		-9.7	C11		-8.9
E11		-9.1	E6		-8.7
H12		-9.1	E13		-8.6
E12		-8.9	E8		-8.6
			C5		-8.5

The molecular docking showed that none of the phthalimide derivatives had a better score than GIG. Nevertheless, these compounds shared some interactions with the complex VEGFR2-GIG. The carboxyl group, common in all the derivatives, is responsible for the hydrogen bonds with Cys917. In addition, C12, E12, and H12 have a biphenyl group that interacts hydrophobically with the same residues as GIG. C11 and E11 with their naphthalene ring interact in the same way as the biphenyl. Another similarity with GIG is the presence of halogen in the structure in the case of E8 and E6. Finally, C5 and E5, which share a nitro group, showed a hydrogen bond with Gly920, in addition to hydrogen bonding with Cys921. Although these results showed that some functional groups could interact with the residues on the binding site of VEGFR2, these compounds showed a lower docking score and a smaller number of non-covalent interactions than GIG. This suggests that these compounds may not target this protein efficiently.

CONCLUSIONS

Forty-three phthalimide derivatives against human cervical cancer (HeLa), human hepatoma (HepG2), murine breast carcinoma (4T1), and murine fibroblast (3T3) cell lines were evaluated. Compounds C16, E11, and E16 were the most antiproliferative agents against HeLa and 4T1 cell lines. In particular, compound H16 had a higher antiproliferative effect against the HepG2 cell line and a null effect against a normal 3T3 cell line. All phthalimide derivatives showed a lower free energy binding than SAH on the active site of DNMT1. However, the compounds showed higher free energy binding than GIG on the active site of VEGFR2. These results, with no correlation between the *in silico* analysis and the biological activity found in phthalimide derivatives, suggest two options: a) another potential drug target is involved in the mechanism of action, and b) poor physicochemical characteristics of compounds do not allow to cross cell membrane and hit the drug target. Therefore, more studies are needed to determine the biological effects that these kinds of compounds have on specific cell lines.

ACKNOWLEDGEMENTS

We wish to express our gratitude to the the Secretaría de Investigación y Posgrado del Instituto Politécnico Nacional for the support granted (SIP-20190295 and SIP-20200491).

REFERENCES

Abdelhaleem, E. F., Abdelhameid, M. K., Kassab, A. E. & Kandeel, M. M. (2018). Design and synthesis of thienopyrimidine urea derivatives with potential cytotoxic and pro-apoptotic activity against breast cancer cell line MCF-7. *European Journal of Medicinal Chemistry*, **143**, 1807-1825. <https://doi.org/10.1016/j.ejmech.2017.10.075>

Al-Abbasi, F. A., Alghamdi, E. A., Baghdadi, M. A., Alamoudi, A. J., El-Halawany, A. M., El-Bassossy, H. M., Aseeri, A. H. & Al-Abd, A. M. (2016). Gingerol Synergizes the

Cytotoxic Effects of Doxorubicin against Liver Cancer Cells and Protects from Its Vascular Toxicity. *Molecules*, **21(7)**, 886. <https://doi.org/10.3390/molecules21070886>

Aliabadi, A., Mohammadi-Farani, A., Hosseinzadeh, Z., Nadri, H., Moradi, A. & Ahmadi, F. (2015). Phthalimide analogs as probable 15-lipoxygenase-1 inhibitors: synthesis, biological evaluation and docking studies. *Daru Journal of Pharmaceutical Sciences*, **23(1)**, 36. <https://doi.org/10.1186/s40199-015-0118-5>

Al-Soud, Y. A. & Al-Masoudi, N. A. (2001). Synthesis and antitumor activity of some new phthalimide analogues. *Pharmazie*, **56**, 372-375. <https://doi.org/10.1002/CHIN.200132132>

Asgatay, S., Champion, C., Marloie, G., Drujon, T., Senamaud-Beaufort, C., Ceccaldi, A., Erdmann, A., Rajavelu, A., Schambel, P., Jeltsch, A., Lequin, O., Karoyan, P., Arimondo, P. B. & Guianvarc'h, D. (2014). Synthesis and evaluation of analogues of N-phthaloyl-L-tryptophan (RG108) as inhibitors of DNA methyltransferase 1. *Journal of Medicinal Chemistry*, **57**, 421-434. <https://doi.org/10.1021/jm401419p>

Bailly, C., Carrasco, C., Joubert, A., Bal, C., Wattez, N., Hildebrand, M.P., Lansiaux, A., Colson, P., Houssier, C., Cacho, M., Ramos, A. & Braña, M.F. (2003). Chromophore-modified bisnaphthalimides: DNA recognition, topoisomerase inhibition, and cytotoxic properties of two mono- and bisfuronaphthalimides. *Biochemistry*, **42**, 4136-4150. <https://doi.org/10.1021/bi027415c>

Chen, Z., Liang, X., Zhang, H., Xie, H., Liu, J., Xu, Y., Zhu, W., Wang, Y., Wang, X., Tan, S., Kuang, D. & Qian, X. (2010). A new class of naphthalimide-based anti-tumor agents that inhibit topoisomerase II and induce lysosomal membrane permeabilization and apoptosis. *Journal of Medicinal Chemistry*, **53**, 2589-2600. <https://doi.org/10.1021/jm100025u>

Grigalius, I. & Petrikaite, V. (2017). Relationship between Antioxidant and Anticancer Activity of Trihydroxyflavones. *Molecules*, **22**, 2169. <https://doi.org/10.3390/molecules22122169>

Kamal, A., Reddy, B. S. N., Reddy, G. S. K. & Ramesh, G. (2002). Design and synthesis of C-8 linked pyrrolobenzodiazepine-naphthalimide hybrids as anti-tumour agents. *Bioorganic and Medicinal Chemistry Letters*, **12**, 1933-1935. [https://doi.org/10.1016/S0960-894X\(02\)00326-8](https://doi.org/10.1016/S0960-894X(02)00326-8)

Kamal, A., Bolla, N. R., Srikanth, P. S. & Srivastava, A. K. (2013). Naphthalimide derivatives with therapeutic characteristics: a patent review. *Expert Opinion on Therapeutic Patents*, **23**, 299-317. <https://doi.org/10.1517/13543776.2013.746313>

Kashif, M., Chacón-Vargas, K. F., López-Cedillo, J. C., Nogueada-Torres, B., Paz-González, A. D., Ramírez-Moreno, E., Agustí, R., Uhrig, M. L., Reyes-Arellano, A., Peralta-Cruz, J., Ashfaq, M. & Rivera, G. (2018). Synthesis, molecular docking and biological evaluation of novel phthaloyl derivatives of 3-amino-3-aryl propionic acids as

- inhibitors of *Trypanosoma cruzi* trans-sialidase. *European Journal of Medicinal Chemistry*, **156**, 252-268. <https://doi.org/10.1016/j.ejmech.2018.07.005>
- Kilic-Kurt, Z., Bakar-Ates, F., Karakas, B. & Kütük, Ö. (2018). Cytotoxic and Apoptotic Effects of Novel Pyrrolo[2,3-d] Pyrimidine Derivatives Containing Urea Moieties on Cancer Cell Lines. *Anticancer Agents in Medicinal Chemistry*, **18**, 1303-1312. <https://doi.org/10.2174/1871520618666180605082026>
- Li, X., Lin, Y., Wang, Q., Yuan, Y., Zhang, H. & Qian, X. (2011). The novel anti-tumor agents of 4-triazol-1, 8-naphthalimides: synthesis, cytotoxicity, DNA intercalation and photocleavage. *European Journal of Medicinal Chemistry*, **46**, 1274-1279. <https://doi.org/10.1016/j.ejmech.2011.01.050>
- Lu, G. Q., Li, X.Y., Mohamed, O. K., Wang, D. & Meng, F. H. (2019). Design, synthesis and biological evaluation of novel uracil derivatives bearing 1, 2, 3-triazole moiety as thymidylate synthase (TS) inhibitors and as potential antitumor drugs. *European Journal of Medicinal Chemistry*, **171**, 282-296. <https://doi.org/10.1016/j.ejmech.2019.03.047>
- Mai, A. & Altucci, L. (2009). Epi-drugs to fight cancer: from chemistry to cancer treatment, the road ahead. *International Journal of Biochemistry & Cell Biology*, **41**, 199-213. <https://doi.org/10.1016/j.biocel.2008.08.020>
- Matsuo, K., Lin, Y. G., Roman, L. D. & Sood A. K. (2010). Overcoming platinum resistance in ovarian carcinoma. *Expert Opinion on Investigational Drugs*, **19**, 1339-54. <https://doi.org/10.1517/13543784.2010.515585>
- Miyachi, H., Ogasawara, A., Azuma, A. & Hashimoto, Y. (1997). Tumor necrosis factor- α production-inhibiting activity of phthalimide analogues on human leukemia THP-1 cells and a structure-activity relationship study. *Bioorganic & Medicinal Chemistry*, **5**, 2095-2102. [https://doi.org/10.1016/S0968-0896\(97\)00148-X](https://doi.org/10.1016/S0968-0896(97)00148-X)
- Morris, G. M., Huey, R., Lindstrom, W., Sanner, M. F., Belew, R. K., Goodsell, D. S. & Olson A. J. (2009). Autodock4 and AutoDockTools4: automated docking with selective receptor flexibility. *Journal of Computational Chemistry*, **16**, 2785-2791. <https://doi.org/10.1002/jcc.21256>
- O'Boyle, N. M., Banck, M., James, C. A., Morley, C., Vandermeersch, T. & Hutchison, G. R. (2011). Open Babel: An open chemical toolbox. *Journal of Cheminformatics*, **3**, 33. <https://doi.org/10.1186/1758-2946-3-33>
- Olazarán-Santibáñez, F., Bandyopadhyay, D., Carranza-Rosales, P., Rivera, G. & Balderas-Rentería, I. (2017a). Stereochemical preference toward oncotarget: Design, synthesis and *in vitro* anticancer evaluation of diastereomeric β -lactams. *Oncotarget*, **8**, 37773-37782. <https://doi.org/10.18632/oncotarget.18077>
- Olazarán, F. E., Rivera, G., Pérez-Vázquez, A. M., Morales-Reyes, C.M., Segura-Cabrera, A. & Balderas-Rentería, I. (2017b). Biological Evaluation *in vitro* and *in silico* of Azetidin-2-one Derivatives as Potential Anticancer Agents. *ACS Medicinal Chemistry Letters*, **8**, 32-37. <https://doi.org/10.1021/acsmchemlett.6b00313>
- Othman, I. M. M., Gad-Elkareem, M. A. M., El-Naggar, M., Nossier, E. S. & Amr, A. E. E. (2019). Novel phthalimide based analogues: design, synthesis, biological evaluation, and molecular docking studies. *Journal of Enzyme Inhibition and Medicinal Chemistry*, **34**(1), 1259-1270. <https://doi.org/10.1016/j.bioorg.2019.102978>
- Pettersen, E. F., Goddard, T. D., Huang, C. C., Couch, G. S., Greenblatt, D.M., Meng, E. C. & Ferrin, T.E. (2004). UCSF Chimera--a visualization system for exploratory research and analysis. *Journal of Computational Chemistry*, **25**, 1605-1612. <https://doi.org/10.1002/jcc.20084>
- Philoppes, J. N. & Lamie, P. F. (2019). Design and synthesis of new benzoxazole/benzothiazole-phthalimide hybrids as antitumor-apoptotic agents. *Bioorganic Chemistry*, **89**, 102978. <https://doi.org/10.1016/j.bioorg.2019.102978>
- Rivera, G., Ahmad-Shah, S. S., Arrieta-Baez, D., Palos, I., Mongue, A. & Sánchez-Torres, L. E. (2017a). Esters of Quinoxaline 1,4-Di-N-oxide with Cytotoxic Activity on Tumor Cell Lines Based on NCI-60 Panel. *Iranian Journal of Pharmaceutical Research*, **16**, 953-965. <https://dx.doi.org/10.22037/ijpr.2017.2065>
- Rivera, G., Andrade-Ochoa, S., Romero, M. S. O., Palos, I., Monge, A. & Sanchez-Torres, L. E. (2017b). Ester of Quinoxaline-7-carboxylate 1,4-di-N-oxide as Apoptosis Inductors in K-562 Cell Line: An *in vitro*, QSAR and DFT Study. *Anticancer Agents in Medicinal Chemistry*, **17**, 682-691. <https://doi.org/10.2174/1871520616666160630175927>
- Salentin, S., Schreiber, S., Haupt, V. J., Adasme, M. F. & Schroeder, M. (2015). PLIP: fully automated protein-ligand interaction profiler. *Nucleic Acids Research*, **43**, W443-447. <https://dx.doi.org/10.1093/nar/gkv315>
- Shiheido, H., Terada, F., Tabata, N., Hayakawa, I., Matsumura, N., Takashima, H., Ogawa, Y., Du, W., Yamada, T., Shoji, M., Sugai, T., Doi, N., Iijima, S., Hattori, Y. & Yanagawa, H. (2012). A phthalimide derivative that inhibits centrosomal clustering is effective on multiple myeloma. *PLoS One*, **7**, e38878. <https://doi.org/10.1371/journal.pone.0038878>
- Siedlecki, P., Garcia Boy, R., Musch, T., Brueckner, B., Suhai, S, Lyko, F. & Zielenkiewicz, P. (2006). Discovery of two novel, small-molecule inhibitors of DNA methylation. *Journal of Medicinal Chemistry*, **49**(2), 678-683. <https://doi.org/10.1021/jm050844z>
- Sundaresan, L., Kumar, P., Manivannan, J., Balaguru, U. M., Kasiviswanathan, D., Veeriah, V., Anishetty, S. & Chatterjee, S. (2019). Thalidomide and Its Analogs Differentially Target Fibroblast Growth Factor Receptors: Thalidomide Suppresses FGFR Gene Expression while Pomalidomide Dampens FGFR2 Activity. *Chemistry Research in Toxicology*, **32**(4), 589-602. <https://doi.org/10.1021/acs.chemrestox.8b00286>

- Trott, O. & Olson, A. J. (2010). AutoDock Vina: improving the speed and accuracy of docking with a new scoring function, efficient optimization, and multithreading. *Journal of Computational Chemistry*, **31**, 455-461. <https://doi.org/10.1002/jcc.21334>
- WHO. World Health Organization (2019). Cancer, Available at <https://www.who.int/cancer/en/>.
- Xie, L., Cui, J., Qian, X., Xu, Y., Liu, J. & Xu, R. (2011). 5-Non-amino aromatic substituted naphthalimides as potential anti-tumor agents: synthesis via suzuki reaction, anti-proliferative activity, and DNA-binding behavior. *Bioorganic & Medicinal Chemistry*, **19**, 961-967. <https://doi.org/10.1016/j.bmc.2010.11.055>
- Yu, N. & Wang, M. (2008). Anticancer drug discovery targeting DNA hypermethylation. *Current Medicinal Chemistry*, **15**, 1350-1375. <https://doi.org/10.2174/092986708784567653>
- Zahran, M. A. H., Abdin, Y. G., Osman, A. M. A., Gamal-Eldeen, A. M., Talaat, R. M. & Pedersen, E. B. (2014). Synthesis and Evaluation of Thalidomide and Phthalimide Esters as Antitumor Agents. *Archiv der Pharmazie*, **347**, 642-649. <https://doi.org/10.1002/ardp.201400073>

In vitro and *in silico* biological evaluation of phthalimide derivatives as antiproliferative agents supplementary material

The supplementary material corresponds to the spectral data of nuclear magnetic resonance, infrared spectrometry of the compounds synthesized by Kashif *et al.*, 2018. Infrared spectra were recorded using OPUS_7.5.18 software with PLATINUM-ATR Bruker Alpha FT-IR spectrometer. NMR data were collected with Bruker Avance 500 spectrometer operating at 500 MHz (¹H), and 126 MHz (¹³C). ¹H proton NMR spectra were obtained in DMSO-*d*₆, with TMS as an internal standard. Chemical shifts are given on the δ scale (ppm). Multiplicities are indicated as follows: s (singlet), d (doublet), t (triplet), q (quartet), m (multiplet) or br (broadened).

H-1: 3-(1,3-dioxoisindolin-2-yl)-3-(4-methoxyphenyl) propanoic acid (B-1)

Yield: 85%, mp 109-1 °C, FTIR (ν cm⁻¹): 3285-2901 (OH), 2988 (CH sp²), 1769_{asym}, 1699_{sym} (NC₂O₂), 1609_{asym}, 1354_{sym} (C=O), 1247 (C-O), 1176 (C-N). ¹H NMR (500 MHz, DMSO-*d*₆): δ 12.37 (s, 1H, COOH), 7.71 (m, 2H, C₆H₄), 7.63 (m, 2H, C₆H₄), 7.41-7.32 (m, 2H, C₆H₄), 6.89-6.87 (m, 2H, C₆H₄), 5.47 (br t, 1H, C₂O₂NH), 3.62 (s, C₆H₄OCH₃), 3.52-3.10 (d, 2H, NHCH₂). ¹³C NMR (126 MHz, DMSO-*d*₆): δ 172.3, 168.3, 168.3, 159.1, 135.3, 135.3, 132.3, 131.5, 131.5, 128.2, 123.5, 123.5, 114.3, 114.1, 55.4, 50.4, 40.1.

H-2: 3-(1,3-dioxoisindolin-2-yl)-3-(*p*-tolyl) propanoic acid (B-2)

Yield: 86%, mp 102-5 °C, FTIR (ν cm⁻¹): 3310-2958 (OH), 3030 (CH sp²), 1770_{asym}, 1699_{sym} (NC₂O₂), 1610_{asym}, 1363_{sym} (C=O), 1215 (C-O), 1169 (C-N). ¹H NMR (500 MHz, DMSO-*d*₆): δ 12.49 (s, 1H, COOH), 7.85 (m, 2H, C₆H₄), 7.78 (m, 2H, C₆H₄), 7.30-7.14 (m, 2H, C₆H₄), 7.10-6.92 (m, 2H, C₆H₄), 5.65 (br t, 1H, C₂O₂NH), 3.51-3.29 (d, 2H, NHCH₂), 2.23 (s, 3H, C₆H₄CH₃). ¹³C NMR (126 MHz, DMSO-*d*₆): δ 172.7, 168.8, 168.8, 144.0, 141.2, 135.2, 134.9, 134.9, 132.3, 131.8, 131.4, 128.4, 123.6, 123.4, 114.2, 114.2, 50.4, 39.6, 22.1.

H-3: 3-(1,3-dioxoisindolin-2-yl)-3-(4-ethylphenyl) propanoic acid (B-3)

Yield: 87%, mp 116-9 °C, FTIR (ν cm⁻¹): 3288-2990 (OH), 3028 (CH sp²), 1770_{asym}, 1700_{sym} (NC₂O₂), 1611_{asym}, 1353_{sym} (C=O), 1215 (C-O), 1170 (C-N). ¹H NMR (500 MHz, DMSO-*d*₆): δ 12.38 (s, 1H, COOH), 7.81 (m, 2H, C₆H₄), 7.62 (m, 2H, C₆H₄), 7.48-7.37 (m, 2H, C₆H₄), 7.10-7.03 (m, 2H, C₆H₄), 5.43 (br t, 1H, C₂O₂NH), 3.43-3.34 (d, 2H, NHCH₂), 2.32 (q, 2H, C₆H₄CH₂CH₃), 1.51 (t, 3H, C₆H₄CH₂CH₃). ¹³C NMR (126 MHz, DMSO-*d*₆): δ 174.2, 168.1, 168.1, 145.2, 141.8, 135.7, 135.4, 129.2, 129.0, 127.9, 127.3, 125.1, 124.5, 52.1, 41.1, 28.2, 14.4.

H-4: 3-(1,3-dioxoisindolin-2-yl)-3-(4-hydroxyphenyl) propanoic acid (B-4)

Yield: 85%, mp 136-8 °C, FTIR (ν cm⁻¹): 3392-2899 (OH), 3058 (CH sp²), 1772_{asym}, 1691_{sym} (NC₂O₂), 1608_{asym}, 1384_{sym} (C=O), 1267 (C-O), 1169 (C-N). ¹H NMR (500 MHz, DMSO-*d*₆): δ 12.43 (s, 1H, COOH), 7.70 (m, 2H, C₆H₄), 7.66 (m, 2H, C₆H₄), 7.20-7.15 (m, 2H, C₆H₄), 6.77-6.69 (m, 2H, C₆H₄), 5.77 (s, 1H, C₆H₄OH), 5.51 (br t, 1H, C₂O₂NH), 3.19-3.10 (d, 2H, NHCH₂). ¹³C NMR (126 MHz, DMSO-*d*₆): δ 173.8, 169.1, 169.1, 160.0, 141.8, 139.3, 136.4, 133.8, 132.0, 130.4, 129.4, 129.1, 119.7, 119.0, 52.1, 41.2.

H-5: 3-(1,3-dioxoisindolin-2-yl)-3-(4-nitrophenyl) propanoic acid (B-5)

Yield: 88%, mp 152-5 °C, FT IR (ν cm⁻¹): 3378-2950 (OH), 3059 (CH sp²), 1773_{asym}, 1702_{sym} (NC₂O₂), 1630_{asym}, 1380_{sym} (C=O), 1545 (NO₂), 1280 (C-O), 1181 (C-N). ¹H NMR (500 MHz, DMSO-d₆): δ 12.54 (s, 1H, COOH), 8.11-8.14 (m, 2H, C₆H₄), 7.98 (m, 2H, C₆H₄), 7.88(m, 2H, C₆H₄), 7.64-7.67 (m, 2H, C₆H₄), 5.41 (br t, 1H, C₂O₂NH), 3.39-3.24 (d, 2H, NHCH₂). ¹³C NMR (126 MHz, DMSO-d₆): δ 171.8, 167.1, 167.1, 150.6, 147.8, 143.4, 137.0, 132.6, 131.7, 131.0, 130.5, 124.2, 123.8, 123.7, 123.4, 51.8, 41.1.

H-6 (B-7) 3-(4-chlorophenyl)-3-(1,3-dioxoisindolin-2-yl) propanoic acid (B-7)

Yield: 85%, mp 158-0 °C, FT IR (ν cm⁻¹): 3402-2945 (OH), 3047 (CH sp²), 1771_{asym}, 1700_{sym} (NC₂O₂), 1626_{asym}, 1352_{sym} (C=O), 1225 (C-O), 1176 (C-N), 793 (C-Cl). ¹H NMR (500 MHz, DMSO-d₆): δ 12.47 (s, 1H, COOH), 7.72-7.67 (m, 4H, C₆H₄), 7.54-7.49 (m, 4H, C₆H₄), 5.39 (br t, 1H, C₂O₂NH), 3.11-2.99 (d, 2H, NHCH₂). ¹³C NMR (126 MHz, DMSO-d₆): δ 172.7, 167.9, 167.9, 146.1, 141.8, 141.5, 138.6, 136.4, 134.1, 134.0, 133.1, 132.4, 129.01, 128.1, 51.4, 40.7.

H-7 (B-6) 3-(1,3-dioxoisindolin-2-yl)-3-(4-fluorophenyl) propanoic acid (B-6)

Yield: 80%, mp 162-4 °C, FT IR (ν cm⁻¹): 3420-2910 (OH), 3058 (CH sp²), 1770_{asym}, 1702_{sym} (NC₂O₂), 1602_{asym}, 1383_{sym} (C=O), 1221 (C-O), 1160 (C-N), 823 (C-F). ¹H NMR (500 MHz, DMSO-d₆): δ 12.39 (s, 1H, COOH), 7.89-7.80 (m, 4H, C₆H₄), 7.31-7.21 (m, 4H, C₆H₄), 5.42 (br t, 1H, C₂O₂NH), 3.22-3.14 (d, 2H, NHCH₂). ¹³C NMR (126 MHz, DMSO-d₆): δ 172.9, 167.6, 167.6, 164.3, 148.1, 142.4, 136.6, 133.1, 130.4, 129.3, 129.1, 124.8, 124.5, 116.9, 116.7, 52.1, 39.6.

H-8 (B-8) 3-(4-bromophenyl)-3-(1,3-dioxoisindolin-2-yl) propanoic acid (B-8)

Yield: 85%, mp 162-4 °C, FT IR (ν cm⁻¹): 3310-2975 (OH), 3050 (CH sp²), 1771_{asym}, 1700_{sym} (NC₂O₂), 1606_{asym}, 1385_{sym} (C=O), 1287 (C-O), 1173 (C-N), 713 (C-Br). ¹H NMR (500 MHz, DMSO-d₆): δ 12.33 (s, 1H, COOH), 7.96 (m, 2H, C₆H₄), 7.86-7.82 (m, 4H, C₆H₄), 7.28-7.22 (m, 2H, C₆H₄), 5.41 (br t, 1H, C₂O₂NH), 3.11-3.08 (d, 2H, NHCH₂). ¹³C NMR (126 MHz, DMSO-d₆): δ 173.1, 166.7, 166.5, 144.1, 135.8, 135.4, 135.1, 132.0, 131.8, 131.8, 130.4, 128.8, 127.6, 125.4, 124.2, 52.5, 41.2.

H-9: 3-(1,3-dioxoisindolin-2-yl)-3-(7-nitro-2,3-dihydrobenzo[b][1,4]dioxin-6-yl) propanoic acid (B-9)

Yield: 78 %, mp 155-8 °C, FT IR (ν cm⁻¹): 3198-2950 (OH), 3064 (CH sp²), 1771_{asym}, 1706_{sym} (NC₂O₂), 1608_{asym}, 1390_{sym} (C=O), 1511 (NO₂), 1257 (C-O), 1159 (C-N). ¹H NMR (500 MHz, DMSO-d₆): δ 12.46 (s, 1H, COOH), 7.88-7.85 (m, 4H, C₆H₄), 7.19 (d, 1H, C₆H₄),

7.10 (d, 1H, C₆H₄), 5.47 (br t, 1H, C₂O₂NH), 4.08 (m, 4H, C₆H₃O₂ C₂H₄), 3.11-3.02 (d, 2H, NHCH₂). ¹³C NMR (126 MHz, DMSO-d₆): δ 173.1, 167.3, 167.3, 152.1, 149.3, 144.1, 140.1, 140.4, 138.4, 132.1, 130.1, 129.1, 125.0, 123.1, 67.1, 67.1, 53.5, 42.1.

H-11: 3-(1,3-dioxoisindolin-2-yl)-3-(naphthalen-2-yl) propanoic acid (B-11)

Yield: 83%, mp 131-4 °C, FT IR (ν cm⁻¹): 3205-2901 (OH), 3071 (CH sp²), 1771_{asym}, 1698_{sym} (NC₂O₂), 1624_{asym}, 1378_{sym} (C=O), 1286 (C-O), 1171 (C-N). ¹H NMR (500 MHz, DMSO-d₆): δ 12.01 (s, 1H, COOH), 8.10-7.88 (m, 3H, C₁₀H₇), 7.86-7.85 (m, 4H, C₆H₄), 7.63-7.61 (m, 2H, C₁₀H₇), 7.21 (d, 1H, C₁₀H₇), 5.63 (br t, 1H, C₂O₂NH), 3.44-3.38 (d, 2H, NHCH₂). ¹³C NMR (126 MHz, DMSO-d₆): δ 172.8, 167.3, 167.3, 145.8, 144.3, 136.9, 133.5, 133.3, 132.6, 132.4, 131.0, 130.8, 130.1, 129.8, 129.7, 129.6, 129.0, 128.7, 128.6, 53.1, 42.5.

H-12: 3-([1,1'-biphenyl]-4-yl)-3-(1,3-dioxoisindolin-2-yl) propanoic acid (B-12)

Yield: 80%, mp 152-5 °C, FT IR (ν cm⁻¹): 3415-2888 (OH), 3031 (CH sp²), 1772_{asym}, 1702_{sym} (NC₂O₂), 1627_{asym}, 1382_{sym} (C=O), 1287 (C-O), 1172 (C-N). ¹H NMR (500 MHz, DMSO-d₆): δ 12.44 (s, 1H, COOH), 7.85-7.83 (s, 4H, C₆H₄), 7.47-7.15 (m, 9H, C₁₂H₉), 5.70 (br t, 1H, C₂O₂NH), 3.40-3.30 (d, 2H, NHCH₂). ¹³C NMR (126 MHz, DMSO-d₆): δ 172.4, 168.1, 168.1, 151.7, 147.6, 133.0, 132.9, 132.8, 132.6, 131.0, 129.9, 129.8, 129.6, 129.5, 129.4, 129.2, 129.0, 128.1, 128.0, 55.1, 44.4.

H-13: 3-(1,3-dioxoisindolin-2-yl)-3-(2-nitrophenyl) propanoic acid (B-13)

Yield: 78%, mp 162-5 °C, FT IR (ν cm⁻¹): 3400-2970 (OH), 3057 (CH sp²), 1772_{asym}, 1703_{sym} (NC₂O₂), 1630_{asym}, 1373_{sym} (C=O), 1571 (NO₂), 1289 (C-O), 1183 (C-N). ¹H NMR (500 MHz, DMSO-d₆): δ 12.62 (s, 1H, COOH), 8.15 (m, 1H, C₆H₄), 7.99-7.92 (m, 4H, C₆H₄), 7.71-7.68 (m, 3H, C₆H₄), 5.77 (br t, 1H, C₂O₂NH), 3.21-3.08 (d, 2H, NHCH₂). ¹³C NMR (126 MHz, DMSO-d₆): δ 173.1, 168.0, 168.0, 152.3, 147.8, 144.0, 138.0, 132.1, 131.2, 130.7, 130.4, 123.5, 123.4, 123.3, 123.2, 53.1, 42.1.

H-14: 3-(1,3-dioxoisindolin-2-yl)-3-(furan-2-yl) propanoic acid (B-14)

Yield: 85%, mp 175-8 °C, FT IR (ν cm⁻¹): 3410-2930 (OH), 3047 (CH sp²), 1772_{asym}, 1713_{sym} (NC₂O₂), 1604_{asym}, 1384_{sym} (C=O), 1286 (C-O), 1182 (C-N). ¹H NMR (500 MHz, DMSO-d₆): δ 11.99 (s, 1H, COOH), 7.86-7.45 (m, 4H, C₆H₄), 7.55 (m, 1H, C₄H₃O), 7.20-6.69 (m, 2H, C₄H₃O), 5.54 (br t, 1H, C₂O₂NH), 3.28-3.02 (d, 2H, NHCH₂). ¹³C NMR (126 MHz, DMSO-d₆): δ 172.2, 167.0, 167.0, 159.0, 145.4, 143.7, 141.7, 135.2, 133.8, 128.6, 123.1, 117.1, 116.3, 53.0, 43.1.

H-16: 3-(1,3-dioxoisindolin-2-yl)-3-(thiophen-2-yl)propanoic acid (B-15)

Yield: 83%, mp 169-1 °C, FTIR (ν cm⁻¹): 3400-2900 (OH), 3058 (CH sp²), 1771_{asym}, 1707_{sym} (NC₂O₂), 1619_{asym}, 1367_{sym} (C=O), 1281 (C-O), 1185 (C-N). ¹H NMR (500 MHz, DMSO-d₆): δ 11.55 (s, 1H, COOH), 7.77-7.40 (m, 4H, C₆H₄), 7.65 (m, 1H, C₄H₃S), 6.88-6.78 (m, 2H, C₄H₃S), 5.44 (br t, 1H, C₂O₂NH), 3.32-3.22 (d, 2H, NHCH₂). ¹³C NMR (126 MHz, DMSO-d₆): δ 172.3, 168.1, 168.1, 141.9, 136.4, 133.2, 131.8, 131.2, 130.1, 129.8, 129.7, 128.9, 128.5, 51.9, 42.7.

E-1: 3-(4-methoxyphenyl)-3-(5-methyl-1,3-dioxoisindolin-2-yl) propanoic acid (D-1)

Yield: 85%, mp 107-9 °C, FTIR (ν cm⁻¹): 3410-2904 (OH), 3042 (CH sp²), 1766_{asym}, 1698_{sym} (NC₂O₂), 1609_{asym}, 1380_{sym} (C=O), 1247 (C-O), 1175 (C-N). ¹H NMR (500 MHz, DMSO-d₆): δ 12.46 (s, 1H, COOH), 7.73 (s, 1H, C₆H₃), 7.71 (s, 1H, C₆H₃), 7.49 (s, 1H, C₆H₃), 7.34-7.32 (m, 2H, C₆H₄), 6.89-6.87 (m, 2H, C₆H₄), 5.58 (br t, 1H, C₂O₂NH), 3.72 (s, C₆H₄OCH₃), 3.44-3.40 (d, 2H, NHCH₂), 2.09 (s, 3H, CH₃). ¹³C NMR (126 MHz, DMSO-d₆): δ 172.3, 168.4, 168.4, 157.2, 140.0, 138.2, 132.2, 131.9, 131.2, 129.1, 129.0, 123.5, 123.5, 118.7, 115.2, 55.6, 50.0, 40.34, 21.03.

E-2: 3-(5-methyl-1,3-dioxoisindolin-2-yl)-3-(p-tolyl) propanoic acid (D-2)

Yield: 88%, mp 116-8 °C, FTIR (ν cm⁻¹): 3400-2888 (OH), 3029 (CH sp²), 1767_{asym}, 1697_{sym} (NC₂O₂), 1614_{asym}, 1379_{sym} (C=O), 1254 (C-O), 1168 (C-N). ¹H NMR (500 MHz, DMSO-d₆): δ 12.43 (s, 1H, COOH), 7.96 (s, 1H, C₆H₃), 7.88 (s, 1H, C₆H₃), 7.65 (s, 1H, C₆H₃), 7.29-7.27 (m, 2H, C₆H₄), 7.13-7.11 (m, 2H, C₆H₄), 5.64 (br t, 1H, C₂O₂NH), 3.22-3.20 (d, 2H, NHCH₂), 2.02 (s, 6H, C₆H₃CH₃, C₆H₄CH₃). ¹³C NMR (126 MHz, DMSO-d₆): δ 172.1, 168.7, 168.7, 142.0, 141.4, 137.4, 135.1, 131.9, 129.6, 129.0, 126.2, 124.9, 123.7, 123.2, 50.4, 40.13, 21.7, 21.5.

E-3: 3-(4-ethylphenyl)-3-(5-methyl-1,3-dioxoisindolin-2-yl) propanoic acid (D-3)

Yield: 87%, mp 114-6 °C, FTIR (ν cm⁻¹): 3415-2940 (OH), 2989 (CH sp²), 1767_{asym}, 1700_{sym} (NC₂O₂), 1617_{asym}, 1380_{sym} (C=O), 1277 (C-O), 1167 (C-N). ¹H NMR (500 MHz, DMSO-d₆): δ 12.17 (s, 1H, COOH), 7.73 (s, 1H, C₆H₃), 7.71 (s, 1H, C₆H₃), 7.62 (s, 1H, C₆H₃), 7.31-7.29 (m, 2H, C₆H₄), 7.17-7.15 (m, 2H, C₆H₄), 5.61 (br t, 1H, C₂O₂NH), 3.44-3.38 (d, 2H, NHCH₂), 2.44 (q, 2H, C₆H₄CH₂CH₃), 2.07 (s, 3H, CH₃), 1.16 (t, 3H, C₆H₄CH₂CH₃). ¹³C NMR (126 MHz, DMSO-d₆): δ 171.9, 167.9, 167.9, 146.1, 143.9, 136.8, 136.3, 128.9, 128.4, 127.8, 127.4, 124.0, 123.5, 50.5, 40.3, 36.3, 28.2, 21.7, 15.9.

E-4: 3-(4-hydroxyphenyl)-3-(5-methyl-1,3-dioxoisindolin-2-yl) propanoic acid (D-4)

Yield: 85%, mp 131-3 °C, FT IR (ν cm⁻¹): 3400-2915 (OH), 3057 (CH sp²), 1764_{asym}, 1700_{sym} (NC₂O₂), 1606_{asym}, 1354_{sym} (C=O), 1254 (C-O), 1170 (C-N NC₂O₂). NMR (500 MHz,

DMSO-d₆): δ 12.47 (s, 1H, COOH), 7.99 (s, 1H, C₆H₃), 7.96 (s, 1H, C₆H₃), 7.76 (s, 1H, C₆H₃), 7.16-7.19 (m, 2H, C₆H₄), 6.87-6.80 (m, 2H, C₆H₄), 6.01 (s, 1H, C₆H₄OH), 5.56 (br t, 1H, C₂O₂NH), 3.32-3.30 (d, 2H, NHCH₂), 2.11 (s, 3H, CH₃). ¹³C NMR (126 MHz, DMSO-d₆): δ 172.4, 168.8, 168.8, 159.2, 143.2, 138.4, 136.1, 133.1, 131.0, 130.0, 129.1, 129.0, 119.4, 119.0, 52.0, 41.2, 21.3.

E-5: 3-(5-methyl-1,3-dioxoisindolin-2-yl)-3-(4-nitrophenyl) propanoic acid (D-5)

Yield: 88%, mp 126-8 °C, FT IR (ν cm⁻¹): 3390-2960 (OH), 3065 (CH sp²), 1765_{asym}, 1701_{sym} (NC₂O₂), 1603_{asym}, 1340_{sym} (C=O), 1540 (NO₂), 1223 (C-O), 1172 (C-N). ¹H NMR (500 MHz, DMSO-d₆): δ 12.68 (s, 1H, COOH), 8.19-8.17 (m, 2H, C₆H₄), 7.98 (s, 1H, C₆H₃), 7.88 (s, 1H, C₆H₃), 7.74 (s, 1H, C₆H₃), 7.66-7.64 (m, 2H, C₆H₄), 5.77 (br t, 1H, C₂O₂NH), 3.30-3.24 (d, 2H, NHCH₂), 2.44 (s, 3H, CH₃). ¹³C NMR (126 MHz, DMSO d₆): δ 172.3, 168.4, 168.4, 149.1, 147.3, 143.1, 136.1, 132.2, 131.1, 130.4, 130.1, 123.6, 123.5, 123.5, 123.4, 50.4, 39.7, 21.7.

E-6: 3-(4-chlorophenyl)-3-(5-methyl-1,3-dioxoisindolin-2-yl) propanoic acid (D-7)

Yield: 85%, mp 133-5 °C, FT IR (ν cm⁻¹): 3400-2970 (OH), 3056 (CH sp²), 1765_{asym}, 1699_{sym} (NC₂O₂), 1614_{asym}, 1378_{sym} (C=O), 1283 (C-O), 1171 (C-N), 839 (C-Cl). ¹H NMR (500 MHz, DMSO-d₆): δ 12.41 (s, 1H, COOH), 7.72 (s, 1H, C₆H₃), 7.69 (s, 1H, C₆H₃), 7.65 (s, 1H, C₆H₃), 7.52-7.50 (m, 2H, C₆H₄), 7.40-7.37 (m, 2H, C₆H₄), 5.65 (br t, 1H, C₂O₂NH), 3.38-3.19 (d, 2H, NHCH₂), 2.43 (s, 3H, CH₃). ¹³C NMR (126 MHz, DMSO-d₆): δ 172.3, 167.2, 167.2, 145.7, 141.4, 141.1, 138.8, 136.2, 134.6, 134.3, 132.1, 132.0, 129.0, 128.4, 50.2, 40.7, 21.8.

E-7: 3-(4-fluorophenyl)-3-(5-methyl-1,3-dioxoisindolin-2-yl) propanoic acid (D-6)

Yield: 89%, mp 136-8 °C, FT IR (ν cm⁻¹): 3388-2899 (OH), 3054 (CH sp²), 1767_{asym}, 1698_{sym} (NC₂O₂), 1604_{asym}, 1355_{sym} (C=O), 1227 (C-O), 1160 (C-N), 884 (C-F). ¹H NMR (500 MHz, DMSO-d₆): δ 12.49 (s, 1H, COOH), 7.85 (s, 1H, C₆H₃), 7.83 (s, 1H, C₆H₃), 7.76 (s, 1H, C₆H₃), 7.30-7.29 (m, 2H, C₆H₄), 7.13-7.11 (m, 2H, C₆H₄), 5.64 (br t, 1H, C₂O₂NH), 3.42-3.32 (d, 2H, NHCH₂), 2.12 (s, 3H, CH₃). ¹³C NMR (126 MHz, DMSO-d₆): δ 171.9, 167.9, 167.4, 162.4, 146.1, 141.1, 132.6, 132.1, 130.4, 129.3, 129.2, 124.6, 124.2, 116.8, 116.7, 50.1, 41.2 21.8.

E-8: 3-(4-bromophenyl)-3-(5-methyl-1,3-dioxoisindolin-2-yl) propanoic acid (D-8)

Yield: 84%, mp 142-5 °C, FT IR (ν cm⁻¹): 3410-2910 (OH), 3055 (CH sp²), 1765_{asym}, 1699_{sym} (NC₂O₂), 1617_{asym}, 1377_{sym} (C=O), 1205 (C-O), 1171 (C-N), 786 (C-Br). ¹H NMR (500 MHz, DMSO-d₆): δ 12.48 (s, 1H, COOH), 7.76 (s, 1H, C₆H₃), 7.71 (s, 1H, C₆H₃), 7.64-7.60 (m, 2H, C₆H₄), 7.51 (s, 1H, C₆H₃), 7.35-7.33 (m, 2H, C₆H₄), 5.62 (br t, 1H, C₂O₂NH), 3.37-3.35 (d, 2H, NHCH₂), 2.44 (s, 3H, CH₃). ¹³C NMR (126 MHz, DMSO-d₆): δ 172.2, 168.1, 168.1, 145.5, 144.9, 136.5, 135.9,

132.2, 131.8, 131.8, 130.4, 129.0, 128.7, 124.6, 124.4, 13.7, 50.5, 40.8, 21.7.

E-9: 3-(5-methyl-1,3-dioxoisindolin-2-yl)-3-(7-nitro-2,3-dihydrobenzo[b][1,4]dioxin-6-yl) propanoic acid (D-9)

Yield: 88%, mp 177-9 °C, FT IR (ν cm⁻¹): 3380-2988 (OH), 3052 (CH sp²), 1764_{asym}, 1703_{sym} (NC₂O₂), 1615_{asym}, 1356_{sym} (C=O), 1521 (NO₂), 1256 (C-O), 1160 (C-N). ¹H NMR (500 MHz, DMSO-d₆): δ 12.42 (s, 1H, COOH), 7.78 (s, 1H, C₆H₃), 7.76 (s, 1H, C₆H₃), 7.62 (s, 1H, C₆H₃), 7.50 (s, 1H, C₆H₃), 7.24 (s, 1H, C₆H₃), 5.54 (br t, 1H, C₂O₂NH), 3.99 (m, 4H, C₆H₃O₂C₂H₄), 3.11-2.99 (d, 2H, NHCH₂), 2.48 (s, 3H, CH₃). ¹³C NMR (126 MHz, DMSO-d₆): δ 171.9, 168.7, 168.7, 154.9, 152.2, 148.9, 143.1, 142.4, 138.4, 130.2, 129.3, 129.1, 126.2, 123.2, 69.4, 69.4, 47.6, 40.3, 21.4.

E-11: 3-(5-methyl-1,3-dioxoisindolin-2-yl)-3-(naphthalen-2-yl) propanoic acid (D-11)

Yield: 88%, mp 142-4 °C, FT IR (ν cm⁻¹): 3390-2947 (OH), 3042 (CH sp²), 1765_{asym}, 1700_{sym} (NC₂O₂), 1616_{asym}, 1354_{sym} (C=O), 1259 (C-O), 1194 (C-N). ¹H NMR (500 MHz, DMSO-d₆): δ 11.37 (s, 1H, COOH), 8.12 (m, 1H, C₈H₇), 8.08 (m, 1H, C₆H₃), 8.06 (m, 1H, C₈H₇), 8.01 (m, 1H, C₈H₇), 8.00 (m, 1H, C₆H₃), 7.99-7.61 (m, 1H, C₈H₇), 7.28 (d, 1H, C₈H₇), 5.871 (br t, 1H, C₂O₂NH), 3.62-3.45 (d, 2H, NHCH₂), 2.38 (s, 3H, CH₃). ¹³C NMR (126 MHz, DMSO-d₆): δ 172.34, 168.4, 168.4, 145.1, 144.7, 136.6, 133.6, 133.1, 132.4, 132.2, 131.3, 130.4, 130.2, 129.8, 129.7, 129.3, 128.9, 128.7, 128.5, 50.5, 40.3, 21.4.

E-12: 3-([1,1'-biphenyl]-4-yl)-3-(5-methyl-1,3-dioxoisindolin-2-yl) propanoic acid (D-12)

Yield: 85%, mp 152-5 °C, FT IR (ν cm⁻¹): 3410-2964 (OH), 3054 (CH sp²), 1767_{asym}, 1700_{sym} (NC₂O₂), 1620_{asym}, 1379_{sym} (C=O), 1279 (C-O), 1169 (C-N). ¹H NMR (500 MHz, DMSO-d₆): δ 12.49 (s, 1H, COOH), 7.85 (s, 1H, C₆H₃), 7.82 (s, 1H, C₆H₃), 7.70 (s, 1H, C₆H₃), 7.54-7.12 (m, 9H, C₁₂H₉), 5.64 (br t, 1H, C₂O₂NH), 3.48-3.30 (d, 2H, NHCH₂), 2.23 (s, 3H, CH₃). ¹³C NMR (126 MHz, DMSO-d₆): δ 172.4, 168.1, 168.1, 150.2, 147.3, 133.1, 132.9, 132.8, 132.7, 131.3, 131.2, 131.0, 130.8, 130.6, 130.5, 130.5, 130.4, 130.1, 130.0, 54.2, 44.4, 22.2.

E-13: 3-(5-methyl-1,3-dioxoisindolin-2-yl)-3-(2-nitrophenyl) propanoic acid (D-13)

Yield: 85%, mp 154-6 °C, FT IR (ν cm⁻¹): 3390-2995 (OH), 3056 (CH sp²), 1765_{asym}, 1704_{sym} (NC₂O₂), 1609_{asym}, 1380_{sym} (C=O), 1571 (NO₂), 1266 (C-O), 1186 (C-N). ¹H NMR (500 MHz, DMSO-d₆): δ 12.68 (s, 1H, COOH), 8.10-8.08 (m, 2H, C₆H₄), 8.00 (s, 1H, C₆H₃), 7.93 (s, 1H, C₆H₃), 7.81 (s, 1H, C₆H₃), 7.71-7.68 (m, 2H, C₆H₄), 5.69 (br t, 1H, C₂O₂NH), 3.21-3.19 (d, 2H, NHCH₂), 2.39 (s, 3H, CH₃). ¹³C NMR (126 MHz, DMSO-d₆): δ 172.1, 168.7, 168.7, 150.3, 147.8, 143.5, 136.5, 132.1, 131.0, 130.3, 130.3, 123.5, 123.4, 123.8, 123.6, 50.7, 40.1, 21.2.

E-14: 3-(furan-2-yl)-3-(5-methyl-1,3-dioxoisindolin-2-yl) propanoic acid (D-14)

Yield: 85%, mp 142-5 °C, FT IR (ν cm⁻¹): 3371-2895 (OH), 3042 (CH sp²), 1769_{asym}, 1703_{sym} (NC₂O₂), 1624_{asym}, 1383_{sym} (C=O), 1250 (C-O), 1169 (C-N). ¹H NMR (500 MHz, DMSO-d₆): δ 12.12 (s, 1H, COOH), 7.71 (s, 1H, C₆H₃), 7.68 (s, 1H, C₆H₃), 7.65 (m, 1H, C₄H₃O), 7.58 (s, 1H, C₆H₃), 7.20-6.69 (m, 2H, C₄H₃O), 5.59 (br t, 1H, C₂O₂NH), 3.31-3.02 (d, 2H, NHCH₂), 2.43 (s, 3H, CH₃). ¹³C NMR (126 MHz, DMSO-d₆): δ 172.1, 168.7, 168.7, 157.0, 145.4, 143.5, 141.8, 135.2, 133.4, 128.5, 123.6, 115.5, 116.3, 50.54, 40.7, 21.4.

E-16: 3-(5-methyl-1,3-dioxoisindolin-2-yl)-3-(thiophen-2-yl) propanoic acid (D-15)

Yield: 85%, mp 141-4 °C, FT IR (ν cm⁻¹): 3410-2907 (OH), 3052 (CH sp²), 1764_{asym}, 1704_{sym} (NC₂O₂), 1613_{asym}, 1380_{sym} (C=O), 1280 (C-O), 1171 (C-N). ¹H NMR (500 MHz, DMSO-d₆): δ 12.12 (s, 1H, COOH), 7.86 (s, 1H, C₆H₃), 7.80 (s, 1H, C₆H₃), 7.65 (m, 1H, C₄H₃S), 7.67 (s, 1H, C₆H₃), 7.11-6.99 (m, 2H, C₄H₃O), 5.61 (br t, 1H, C₂O₂NH), 3.34-3.22 (d, 2H, NHCH₂), 2.40 (s, 3H, CH₃). ¹³C NMR (126 MHz, DMSO-d₆): δ 172.3, 168.1, 168.1, 141.9, 136.4, 133.2, 130.1, 130.0, 129.8, 129.4, 129.1, 128.5, 128.4, 51.9, 41.0, 21.2.

C-1: 2-(2-carboxy-1-(4-methoxyphenyl)ethyl)-1,3-dioxoisindoline-5-carboxylic acid (C-1)

Yield: 85%, mp 100-2 °C, FT IR (ν cm⁻¹): 3398-2950 (OH), 3071 (CH sp²), 1775_{asym}, 1702_{sym} (NC₂O₂), 1605_{asym}, 1359_{sym} (C=O), 1245 (C-O), 1172 (C-N). ¹H NMR (500 MHz, DMSO-d₆): δ 13.25 (s, 1H, COOH), 11.50 (s, 1H, C₆H₃COOH) 8.33 (s, 1H, C₆H₃), 8.30 (s, 1H, C₆H₃), 8.10 (s, 1H, C₆H₃), 7.85-7.83 (m, 2H, C₆H₄), 7.52-7.50 (m, 2H, C₆H₄), 5.89 (br t, 1H, C₂O₂NH), 3.80 (s, 3H, C₆H₄OCH₃), 3.51-3.45 (d, 2H, NHCH₂). ¹³C NMR (126 MHz, DMSO-d₆): δ 172.3, 169.9, 168.3, 168.3, 162.1, 141.2, 139.7, 136.2, 136.8, 135.6, 133.1, 130.9, 130.6, 130.5, 119.8, 119.6, 60.2, 55.1, 44.3.

C-2: 2-(2-carboxy-1-(p-tolyl)ethyl)-1,3-dioxoisindoline-5-carboxylic acid (C-2)

Yield: 85%, mp 112-5 °C, FT IR (ν cm⁻¹): 3398-2950 (OH), 3071 (CH sp²), 1775_{asym}, 1702_{sym} (NC₂O₂), 1605_{asym}, 1359_{sym} (C=O), 1245 (C-O), 1172 (C-N). ¹H NMR (500 MHz, DMSO-d₆): δ 13.30 (s, 1H, COOH), 11.57 (s, 1H, C₆H₃COOH) 8.31 (s, 1H, C₆H₃), 8.29 (s, 1H, C₆H₃), 8.15 (s, 1H, C₆H₃), 7.95-7.93 (m, 2H, C₆H₄), 7.71-7.69 (m, 2H, C₆H₄), 5.88 (br t, 1H, C₂O₂NH), 3.56-3.44 (d, 2H, NHCH₂), 2.49 (s, 3H, C₆H₄CH₃). ¹³C NMR (126 MHz, DMSO-d₆): δ 172.9, 169.8, 167.8, 167.8, 142.5, 141.5, 140.8, 140.6, 139.5, 136.6, 134.6, 134.3, 133.3, 132.0, 128.6, 128.4, 55.2, 44.0, 25.8.

C-3: 2-(2-carboxy-1-(4-ethylphenyl)ethyl)-1,3-dioxoisindoline-5-carboxylic acid (C-3)

Yield: 85%, mp 116-8 °C, FT IR (ν cm⁻¹): 3415-2970 (OH), 3033 (CH sp²), 1774_{asym}, 1695_{sym} (NC₂O₂), 1625_{asym}, 1380_{sym}

(C=O), 1248(C-O), 1164(C-N). ¹H NMR (500 MHz, DMSO-*d*₆) δ 13.23 (s, 1H, COOH), 11.49 (s, 1H, C₆H₃COOH), 8.33 (s, 1H, C₆H₃), 8.30 (s, 1H, C₆H₃), 8.10 (s, 1H, C₆H₃), 7.99-7.97 (m, 2H, C₆H₄), 7.81-7.79 (m, 2H, C₆H₄), 5.90 (br t, 1H, C₂O₂NH), 3.44-3.38 (d, 2H, NHCH₂), 2.38 (q, 2H, C₆H₄CH₂CH₃), 1.27 (t, 3H, C₆H₄CH₂CH₃). ¹³C NMR (126 MHz, DMSO-*d*₆): δ 172.1, 169.1, 168.1, 168.1, 142.9, 141.1, 140.3, 140.1, 139.3, 136.4, 134.1, 134.0, 133.5, 129.9, 129.6, 128.3, 54.9, 44.3, 31.7, 20.1.

C-4: 2-(2-carboxy-1-(4-hydroxyphenyl)ethyl)-1,3-dioxoisindoline-5-carboxylic acid (C-4)

Yield: 87%, mp 128-0 °C, FT IR (ν cm⁻¹): 3410-2905 (OH), 3011 (CH sp²), 1763_{asym}, 1702_{sym} (NC₂O₂), 1619_{asym}, 1379_{sym} (C=O), 1238(C-O), 1170(C-N). ¹H NMR (500 MHz, DMSO-*d*₆) δ 12.99 (s, 1H, COOH), 11.3 (s, 1H, C₆H₃COOH), 8.31 (s, 1H, C₆H₃), 8.30 (s, 1H, C₆H₃), 8.01 (s, 1H, C₆H₃), 7.87-7.85 (m, 2H, C₆H₄), 7.25-7.15 (m, 2H, C₆H₄), 5.81 (s, 1H, C₆H₄OH), 5.62 (br t, 1H, C₂O₂NH), 3.42-3.31 (d, 2H, NHCH₂). ¹³C NMR (126 MHz, DMSO-*d*₆): δ 172.3, 169.0, 167.2, 167.2, 157.4, 139.9, 138.8, 134.8, 133.4, 132.7, 132.5, 129.0, 123.2, 122.1, 115.7, 115.2, 50.1, 39.8.

C-5: 2-(2-carboxy-1-(4-nitrophenyl)ethyl)-1,3-dioxoisindoline-5-carboxylic acid (C-5)

Yield: 85%, mp 154-6 °C, FT IR (ν cm⁻¹): 3395-2926 (OH), 3017 (CH sp²), 1775_{asym}, 1698_{sym} (NC₂O₂), 1619_{asym}, 1363_{sym} (C=O), 1516 (NO₂), 1281 (C-O), 1172 (C-N). ¹H NMR (500 MHz, DMSO-*d*₆): δ 13.10 (s, 1H, COOH), 11.5 (s, 1H, C₆H₃COOH), 8.35 (s, 1H, C₆H₃), 8.33 (s, 1H, C₆H₃), 8.22-8.18 (m, 2H, C₆H₄), 8.05 (s, 1H, C₆H₃), 7.96-7.87 (m, 2H, C₆H₄), 5.89 (br t, 1H, C₂O₂NH), 3.54-3.28 (d, 2H, NHCH₂). ¹³C NMR (126 MHz, DMSO-*d*₆): δ 171.7, 169.8, 167.6, 167.6, 148.7, 138.8, 138.1, 136.2, 135.3, 135.2, 134.2, 134.0, 133.0, 132.1, 131.0, 123.3, 50.2, 40.47.

C-6: 2-carboxy-1-(4-chlorophenyl)ethyl)-1,3-dioxoisindoline-5-carboxylic acid (C-7)

Yield: 88%, mp 142-6 °C, FT IR (ν cm⁻¹): 3467-2900 (OH), 3037 (CH sp²), 1775_{asym}, 1701_{sym} (NC₂O₂), 1626_{asym}, 1359_{sym} (C=O), 1275 (C-O), 1154 (C-N), 725 (C-Cl). ¹H NMR (500 MHz, DMSO-*d*₆) δ 13.10 (s, 1H, COOH), 11.54 (s, 1H, C₆H₃COOH), 8.32 (s, 1H, C₆H₃), 8.19 (s, 1H, C₆H₃), 8.07 (s, 1H, C₆H₃), 7.86-7.80 (m, 2H, C₆H₄), 7.45-7.36 (m, 2H, C₆H₄), 5.71 (br t, 1H, C₂O₂NH), 3.47-3.31 (d, 2H, NHCH₂). ¹³C NMR (126 MHz, DMSO-*d*₆): δ 173.1, 171.3, 169.4, 169.4, 148.3, 141.9, 140.2, 139.5, 138.6, 138.0, 135.1, 134.8, 134.6, 134.5, 133.8, 130.2, 54.7, 44.6.

C-7: 2-(2-carboxy-1-(4-fluorophenyl)ethyl)-1,3-dioxoisindoline-5-carboxylic acid (C-6)

Yield: 86%, mp 165-8 °C, FT IR (ν cm⁻¹): 3420-2898 (OH), 3013 (CH sp²), 1776_{asym}, 1695_{sym} (NC₂O₂), 1624_{asym}, 1336_{sym} (C=O), 1280(C-O), 1160(C-N), 790(C-F). ¹H NMR (500 MHz, DMSO-*d*₆) δ 13.04 (s, 1H, COOH), 11.57 (s, 1H, C₆H₃COOH)

8.34 (s, 1H, C₆H₃), 8.20 (s, 1H, C₆H₃), 8.01 (s, 1H, C₆H₃), 7.77-7.61 (m, 2H, C₆H₄), 7.40-7.32 (m, 2H, C₆H₄), 5.71 (br t, 1H, C₂O₂NH), 3.48-3.30 (d, 2H, NHCH₂). ¹³C NMR (126 MHz, DMSO-*d*₆): δ 172.1, 169.1, 167.2, 167.2, 161.1, 140.2, 136.1, 135.9, 135.2, 134.7, 133.8, 133.6, 132.2, 116.8, 115.9, 50.5, 40.3.

C-8: 2-(1-(4-bromophenyl)-2-carboxyethyl)-1,3-dioxoisindoline-5-carboxylic acid (C-8)

Yield: 80%, mp 166-8 °C, FT IR (ν cm⁻¹): 3430-2940 (OH), 3028 (CH₂ sp²), 1775_{asym}, 1696_{sym} (NC₂O₂), 1637_{asym}, 1358_{sym} (C=O), 1280(C-O), 1169(C-N), 699(C-Br). ¹H NMR (500 MHz, DMSO-*d*₆) δ 13.30 (s, 1H, COOH), 11.53 (s, 1H, C₆H₃COOH), 8.33 (m, 1H, C₆H₃), 8.20 (s, 1H, C₆H₃), 8.16 (m, 1H, C₆H₃), 7.96-7.88 (m, 2H, C₆H₄), 7.58-7.39 (m, 2H, C₆H₄), 5.64 (br t, 1H, C₂O₂NH), 3.46-3.31 (d, 2H, NHCH₂). ¹³C NMR (126 MHz, DMSO-*d*₆): δ 172.3, 169.9, 166.8, 166.8, 143.2, 138.5, 137.5, 137.0, 136.0, 135.4, 133.0, 132.4, 132.0, 131.9, 130.5, 129.5, 50.5, 40.3.

C-9: 2-(2-carboxy-1-(7-nitro-2,3-dihydrobenzo[b][1,4]dioxin-6-yl)ethyl)-1,3-dioxoisindoline-5-carboxylic acid (C-9)

Yield: 84%, mp 172-4 °C, FT IR (ν cm⁻¹): 3421-2977 (OH), 2999 (CH₂ sp²), 1775_{asym}, 1702_{sym} (NC₂O₂), 1606_{asym}, 1360_{sym} (C=O), 1256 (C-O), 1157 (C-N). ¹H NMR (500 MHz, DMSO-*d*₆): δ 12.42 (s, 1H, COOH), 11.48 (s, 1H, C₆H₃COOH), 8.34 (s, 1H, C₆H₃), 8.31 (s, 1H, C₆H₃), 8.01 (s, 1H, C₆H₃), 7.77 (s, 1H, C₆H₃), 7.68 (s, 1H, C₆H₃), 5.71 (br t, 1H, C₂O₂NH), 4.19 (m, 4H, C₆H₃O₂C₂H₄), 3.66-3.12 (d, 2H, NHCH₂). ¹³C NMR (126 MHz, DMSO-*d*₆): δ 172.3, 169.0, 167.8, 167.8, 156.9, 152.8, 149.1, 143.9, 142.8, 139.3, 131.1, 129.3, 129.1, 126.2, 124.3, 69.8, 69.8, 49.3, 40.9.

C-10: 2-(2-carboxy-1-(2,3-dihydrobenzo[b][1,4]dioxin-6-yl)ethyl)-1,3-dioxoisindoline-5-carboxylic acid (C-10)

Yield: 80%, mp 161-4 °C, FT IR (ν cm⁻¹): 3421-2929 (OH), 2990 (CH₂ sp²), 1763_{asym}, 1697_{sym} (NC₂O₂), 1619_{asym}, 1356_{sym} (C=O), 1250 (C-O), 1147 (C-N). ¹H NMR (500 MHz, DMSO-*d*₆): δ 12.98 (s, 1H, COOH), 11.38 (s, 1H, C₆H₃COOH), 8.34 (s, 1H, C₆H₃), 8.29 (s, 1H, C₆H₃), 8.09 (s, 1H, C₆H₃), 7.46 (s, 1H, C₆H₃), 7.19 (s, 1H, C₆H₃), 7.10 (s, 1H, C₆H₃), 5.61 (br t, 1H, C₂O₂NH), 4.20 (m, 4H, C₆H₃O₂C₂H₄), 3.42-3.22 (d, 2H, NHCH₂). ¹³C NMR (126 MHz, DMSO-*d*₆): δ 172.4, 169.4, 168.1, 168.1, 147.2, 146.9, 143.6, 134.9, 133.0, 131.9, 130.8, 129.6, 123.1, 120.4, 119.2, 116.0, 64.8, 64.8, 50.1, 40.0.

C-11: 2-(2-carboxy-1-(naphthalen-2-yl)ethyl)-1,3-dioxoisindoline-5-carboxylic acid (C-11)

Yield: 85%, mp 142-4 °C, FT IR (ν cm⁻¹): 3400-2947 (OH), 3062 (CH₂ sp²), 1776_{asym}, 1699_{sym} (NC₂O₂), 1622_{asym}, 1362_{sym} (C=O), 1255 (C-O), 1173 (C-N). ¹H NMR (500 MHz, DMSO-*d*₆): δ 13.27 (s, 1H, COOH), 11.56 (s, 1H, C₆H₃COOH), 8.33 (m, 1H, C₆H₃), 8.30 (m, 1H, C₆H₃), 8.01 (m, 1H, C₆H₃), 7.99 (m, 1H, C₈H₇), 7.82 (m, 1H, C₈H₇), 7.61 (m, 1H, C₈H₇), 7.58-7.45 (m, 1H, C₈H₇), 7.28 (d,

¹H, C₈H₇), 5.89 (brt, 1H, C₂O₂NH), 3.57-3.49 (d, 2H, NHCH₂). ¹³C NMR (126 MHz, DMSO-d₆): δ 172.3, 168.9, 167.2, 167.2, 144.3, 136.6, 136.5, 136.4, 136.3, 135.6, 135.5, 134.8, 133.4, 132.8, 132.0, 130.9, 129.1, 128.2, 126.0, 124.3, 50.9, 40.3.

C-12: 2-(1-([1,1'-biphenyl]-4-yl)-2-carboxyethyl)-1,3-dioxoisindoline-5-carboxylic acid (C-12)

Yield: 87%, mp 156-8 °C, FTIR (ν cm⁻¹): 3422-3120 (OH), 3007 (CH₂ sp²), 1775_{asym}, 1698_{sym} (NC₂O₂), 1625_{asym}, 1360_{sym} (C=O), 1223 (C-O), 1170 (C-N). ¹H NMR (500 MHz, DMSO-d₆): δ 13.13 (s, 1H, COOH), 11.58 (s, 1H, C₆H₃COOH), 8.36 (m, 1H, C₆H₃), 8.22 (s, 1H, C₆H₃), 8.01 (s, 1H, C₆H₃), 7.79-7.31 (m, 9H, C₁₂H₉), 5.77 (br t, 1H, C₂O₂NH), 3.50-3.39 (d, 2H, NHCH₂). ¹³C NMR (126 MHz, DMSO-d₆): δ 172.3, 169.3, 166.8, 166.8, 143.2, 142.2, 140.5, 140.4, 139.6, 138.2, 136.9, 136.5, 135.5, 134.8, 133.7, 133.5, 132.2, 129.6, 128.3, 127.3, 126.5, 124.5, 50.5, 40.3.

C-13: 2-(2-carboxy-1-(2-nitrophenyl)ethyl)-1,3-dioxoisindoline-5-carboxylic acid (C-13)

Yield: 85%, mp 131-4 °C, FT IR (ν cm⁻¹): 3395-2926 (OH), 3017 (CH sp²), 1775_{asym}, 1698_{sym} (NC₂O₂), 1619_{asym}, 1363_{sym} (C=O), 1516 (NO₂), 1281 (C-O), 1172 (C-N). ¹H NMR (500 MHz, DMSO-d₆): δ 13.09 (s, 1H, COOH), 11.58 (s, 1H, C₆H₃COOH), 8.33 (s, 1H, C₆H₃), 8.30 (s, 1H, C₆H₃), 8.20-8.18 (m, 2H, C₆H₄), 8.10 (s, 1H, C₆H₃), 7.99-7.92 (m, 2H, C₆H₄), 5.82 (br t, 1H, C₂O₂NH), 3.48-3.40 (d, 2H, NHCH₂). ¹³C NMR (126 MHz, DMSO-d₆): δ 172.2, 169.0, 167.6, 167.6, 149.7,

138.6, 138.3, 136.4, 135.8, 135.4, 134.3, 134.0, 133.8, 132.6, 131.7, 123.2, 51.3, 41.4.

C-14: 2-(2-carboxy-1-(furan-2-yl)ethyl)-1,3-dioxoisindoline-5-carboxylic acid (C-14)

Yield: 80%, mp 151-4 °C, FTIR (ν cm⁻¹): 3421-2899 (OH), 2990 (CH₂ sp²), 1762_{asym}, 1720_{sym} (NC₂O₂), 1620_{asym}, 1357_{sym} (C=O), 1255 (C-O), 1177 (C-N). ¹H NMR (500 MHz, DMSO-d₆): δ 12.60 (s, 1H, COOH), 11.10 (s, 1H, C₆H₃COOH), 8.32 (s, 1H, C₆H₃), 8.24 (s, 1H, C₆H₃), 7.58 (s, 1H, C₆H₃), 7.77 (m, 1H, C₄H₃O), 7.01-6.69 (m, 2H, C₄H₃O), 5.59 (br t, 1H, C₂O₂NH), 3.31-3.02 (d, 2H, NHCH₂), 2.43 (s, 3H, C₆H₃CH₃). ¹³C NMR (126 MHz, DMSO-d₆): δ 172.0, 169.3, 168.1, 168.1, 156.0, 146.4, 143.9, 142.1, 137.2, 135.4, 129.7, 124.5, 119.4, 117.1, 50.9, 40.9.

C-16: 2-(2-carboxy-1-(thiophen-2-yl)ethyl)-1,3-dioxoisindoline-5-carboxylic acid (C-15)

Yield: 88%, mp 139-1 °C, FTIR (ν cm⁻¹): 3402-2945 (OH), 3010 (CH₂ sp²), 1763_{asym}, 1698_{sym} (NC₂O₂), 1618_{asym}, 1359_{sym} (C=O), 1259 (C-O), 1175 (C-N). ¹H NMR (500 MHz, DMSO-d₆): δ 11.99 (s, 1H, COOH), 10.10 (s, 1H, C₆H₃COOH), 8.34 (s, 1H, C₆H₃), 8.31 (s, 1H, C₆H₃), 8.11 (s, 1H, C₆H₃), 7.51 (m, 1H, C₄H₃S), 7.01-6.99 (m, 2H, C₄H₃S), 5.69 (br t, 1H, C₂O₂NH), 3.40-3.31 (d, 2H, NHCH₂). ¹³C NMR (126 MHz, DMSO-d₆): δ 172.3, 169.4, 168.0, 168.0, 141.0, 136.7, 133.3, 130.1, 129.8, 129.7, 129.4, 129.1, 128.8, 128.3, 51.3, 41.6.